

Spatio-temporal variability of zooplankton standing stock in eastern Arabian Sea inferred from ADCP backscatter measurements

Ranjan Kumar Sahu, P. Amol, D.V. Desai, S.G. Aparna, D. Shankar

August 2, 2024

Abstract

We use acoustic Doppler current profiler (ADCP) backscatter measurements to map the spatio-temporal variation of zooplankton standing stock in the eastern Arabian Sea (EAS). The ADCP moorings were deployed at seven locations on the continental slope off the west coast of India; we use data from October 2017 to December 2023. The 153.3 kHz ADCP uses backscatter from sediments or organisms such as copepods, ctenophores, salps and amphipods greater than 1 cm to calculate current profile. The backscatter is obtained from echo intensity using RSSI conversion factor after doing necessary calibrations. The conversion from backscatter to biomass is based on volumetric zooplankton sampling at the respective locations. Analysis of the data over 24 – 120 m shows that the backscatter and zooplankton biomass decrease from the upper ocean (215 m g^{-3} biomass contour) to the lower depths. Changes are observed in the seasonal variation of the monthly

¹² climatology of zooplankton standing stock (integral of the biomass over 24 – 120 m water column)
¹³ as we move to poleward along the slope in EAS. The range of variation of standing stock is lowest
¹⁴ at Kanyakumari, followed by Okha, which lie at the southern and northern boundary of the EAS,
¹⁵ respectively. Complementary variables are used to explain the processes leading to growth or decay
¹⁶ of zooplankton biomass.

₁₇ **1 Introduction**

₁₈ **1.1 Background**

₁₉ Zooplankton plays a vital role in food web of pelagic ecosystem by enabling the hierarchical trans-
₂₀ port of organic matter from primary producers to higher trophic levels impacting the fish population
₂₁ and the carbon pump of the deep ocean [Ohman and Hirche, 2001, Le Qu et al., 2016]. They are
₂₂ presumably the largest migrating organisms in terms of biomass [Hays, 2003] which occurs in diel
₂₃ vertical migration (DVM). Zooplanktons depend not only on phytoplankton but other environ-
₂₄ mental parameters (e.g. Mixed layer depth, insolation, Oxygen, thermocline, nutrient availability,
₂₅ chlorophyll concentration and daily primary production). The biological productivity of the ocean
₂₆ is essentially connected with physics and chemistry [Subrahmanyam, 1959, Ryther et al., 1966,
₂₇ Qasim, 1977, Nair, 1970, Banse, 1995, McCreary et al., 2009, Vijith et al., 2016, Amol et al., 2020].
₂₈ The dynamic ocean results in varying physico-chemical properties, leading to bloom and growth of
₂₉ planktons in favourable conditions. The changes are strongly influenced by the seasonal cycle in
₃₀ the North Indian Ocean (NIO; north of 5 °N of Indian Ocean). The eastern boundary of Arabian
₃₁ Sea contains the West India Coastal Current (WICC; [Patil et al., 1964, Ramamirtham and Murty,
₃₂ 1965, Banse, 1968, Shetye et al., 1991, McCreary Jr et al., 1993, Shankar and Shetye, 1997, Shetye
₃₃ and Gouveia, 1998, Maheswaran et al., 2000, Amol et al., 2014, Chaudhuri et al., 2020, 2021])
₃₄ which reverses seasonally, flowing poleward (equatorward) during November to February (June to
₃₅ September).
₃₆ The direct consequence of this reversal is the seasonal cycle of thermocline, oxycline and thick-
₃₇ ness of mixed Layer Depth (MLD) induced by upwelling favourable conditions in summer and down-
₃₈ welling favourable conditions in winter in eastern Arabian Sea (EAS). Further, the phytoplankton

39 biomass and chlorophyll concentration changes with the season [Subrahmanyam and Sarma, 1960,
40 Banse, 1968, Lévy et al., 2007, Vijith et al., 2016]. Upwelling in summer monsoon leads to maximum
41 chlorophyll growth in the entire EAS [Banse, 1968, Banse and English, 2000, McCreary et al., 2009,
42 Hood et al., 2017, Shi and Wang, 2022]. During winter monsoon, the convective mixing induced
43 winter mixed layer [Shetye et al., 1992, Madhupratap et al., 1996b, Lévy et al., 2007, Vijith et al.,
44 2016, Shankar et al., 2016, Keerthi et al., 2017, Shi and Wang, 2022] results in winter chlorophyll
45 peak in northern EAS (NEAS) while the downwelling Rossby waves modulate chlorophyll along
46 the southern EAS (SEAS) albeit limited to coast and islands [Amol et al., 2020]. (For a detailed
47 description on EAS division, please refer figure 1 of [Shankar et al., 2019].

48 The zooplankton grazing peak is instantaneous with no time delay from peak phytoplankton
49 production [Li et al., 2000], but its population growth lags [Rehim and Imran, 2012, Almén and
50 Tamelander, 2020] depending on its gestation period and other limiting aspects. While some studies
51 suggest that the peak timing of zooplankton may not change in parallel with phytoplankton blooms
52 [Winder and Schindler, 2004], others indicate that lag exists between primary production and the
53 transfer of energy to higher trophic levels [Brock and McClain, 1992, Brock et al., 1991]. A recent
54 work [Aparna et al., 2022] had shown that peak zooplankton population may never occur even
55 with a bloom in phytoplankton such as in SEAS, leading to the collapse of ecological models and
56 succeeding food webs of higher trophic levels.

57 The conventional zooplankton measurements, where only few snapshot/s of the event is captured
58 gives an incoherent or incomplete understanding in terms of spatio-temporal variation of zooplank-
59 ton [Ramamurthy, 1965, Piontkovski et al., 1995, Madhupratap et al., 1992, 1996a, Wishner et al.,
60 1998, Khandagale et al., 2022] as much information is revealed by later studies [Jyothibabu et al.,
61 2010, Vijith et al., 2016, Shankar et al., 2019, Aparna et al., 2022] using high resolution data.

62 Calibrated acoustic instruments such as Acoustic Doppler Current Profiler (ADCP) along with rel-
63 evant data can be utilised to understand small scale variability [Nair et al., 1999, Edvardsen et al.,
64 Smith and Madhupratap, 2005, Smeti et al., 2015, Kang et al., 2024], the complex interplay
65 between the physico-chemical parameters and ecosystem [Jiang et al., 2007, Potiris et al., 2018,
66 Shankar et al., 2019, Aparna et al., 2022, Nie et al., 2023], the zooplankton migration [Inoue et al.,
67 2016, Ursella et al., 2018, 2021] and their seasonal to annual variation [Jiang et al., 2007, Hobbs
68 et al., 2021, Liu et al., 2022, Aparna et al., 2022].

69 **1.2 ADCP backscatter and zooplankton biomass**

70 At present, there are two types of acoustic samplers: non-calibrated single frequency acoustic profiler
71 such as ADCP or calibrated multi and mono frequency acoustic profilers such as zooplankton
72 acoustic profiler (ZAP) and Tracor acoustic profiling system(TAPS). The use of acoustics as a
73 proxy for zooplankton biomass estimation can be traced to [Pieper, 1971, Sameoto and Paulowich,
74 1977] and earlier studies which used echograms to approximate the large-scale horizontal extents
75 [Barraclough et al., 1969], and small scale vertical extent [McNaught, 1968]. The relationship
76 between backscatter and the abundance and size of zooplankton was described by [Greenlaw, 1979]
77 wherein it was pointed out that single frequency backscatter can be used to estimate abundance if
78 mean zooplankton size is known. This paved the way for use of single frequency acoustic profiler. A
79 drastic increase in study temporal and spatial variation of zooplankton biomass using backscatter-
80 proxy came in 1990s by introduction of high frequency echo sounders, with studies [Flagg and Smith,
81 1989, Wiebe et al., 1990, Batchelder et al., 1995, Greene et al., 1998, Rippeth and Simpson, 1998]
82 methodically showing acoustic backscatter estimated zooplankton biomass in various shelf and slope
83 locations around North Atlantic, North pacific location. The foundation for further research that

84 investigated the potential of acoustic backscatter from ADCPs and multi frequency echo sounders
85 in assessing zooplankton biomass and comprehending zooplankton dynamics in diverse maritime
86 habitats was established by these initial explorative experiments.

87 Acoustic backscatter and zooplankton biomass have been better understood as a result of tech-
88 nological and methodological developments over time. Net sampling augmented ADCP backscatter
89 have been used to study DVM and the spatial and temporal variability of zooplankton biomass by
90 [Cisewski et al., 2010, Hamilton et al., 2013, Smeti et al., 2015, Guerra et al., 2019] in different
91 marine regions, such as the Southwestern Pacific, the Lazarev Sea in Antarctica and the Corsica
92 Channel in the north-western Mediterranean Sea. The zooplankton biomass variation in the Ara-
93 bian sea has been studied during JGOFS programme in 1990s [Herring et al., 1998, Nair et al.,
94 1999, Fielding et al., 2004, Smith and Madhupratap, 2005]. However, their studies were limited to
95 the cruise duration as vessel mounted ADCPs were predominantly used; hence long-term data was
96 sparsely produced. The first such study to fully exploit the immense potential of ADCPs in EAS
97 was carried out by [Aparna et al., 2022] using ADCP moorings deployed on continental slopes off
98 the Indian west coasts [Amol et al., 2014, Chaudhuri et al., 2020].

99 1.3 Objective and scope of the manuscript

100 A network of ADCPs has been installed off the continental slope and shelf on the west coast of
101 India. This ADCPs have enabled a rigorous view of intraseasonal to seasonal scale variability [Amol
102 et al., 2014, Chaudhuri et al., 2020]. Initially a network of 4 ADCPs (off Mumbai, Goa, Kollam and
103 Kanyakumari) on continental slope, it has been extended to include 3 more moorings (off Okha from
104 2018, Jaigarh and Udupi from 2017). In the recent study [Aparna et al., 2022] have used ADCP
105 moorings off Mumbai, Goa and Kollam to explain the temporal variability of zooplankton biomass.

106 The study showed that the zooplankton peaks (and troughs) is not only non-uniform in latitude but
107 also heavily influenced by the oxygen minimum zone, MLD and the seasonal upwelling/downwelling
108 conditions. Stark contrast in the phytoplankton bloom and subsequence growth of zooplankton or
109 the lack thereof was observed in the EAS regimes.

110 We build upon the existing work by extending to include the newly incorporated ADCPs so as to
111 have a better understanding in the latitudinal variation of zooplankton biomass in EAS. The paper
112 is organized as follows; datasets and methods employed are described in detail in Section 2. Section
113 3 describes the observed climatology of zooplankton biomass and standing stock. A comparison is
114 drawn to the results of previous studies at the overlapping mooring sites. Further, the seasonal cycle
115 of zooplankton biomass and standing stock is discussed. The role of mixed layer depth, net primary
116 production, sea surface temperature, wind forcing and circulation in determining the biomass is
117 discussed in results section 4, with conclusion in section 5.

118 2 Data and methods

119 The backscatter data from ADCP and the zooplankton samples collected from the periphery of
120 mooring is described in this section. The methodology followed in processing ADCP data and
121 estimation of backscatter and subsequently the zooplankton biomass is discussed. The backscatter
122 derived from the echo intensity of the seven ADCP mooring deployed on the continental slope off
123 the Indian west coast is the primary data we have use in this manuscript. The moorings details are
124 summarised in [Table 1](#). In situ biomass data from volumetric zooplankton samples are used to val-
125 idate and correlate with backscatter. The chlorophyll data is obtained from marine.copernicus.eu.
126 In addition, we have used the monthly climatology of temperature and salinity [[Chatterjee et al.,](#)
127 [2012](#)] and the net primary productivity from MODIS (Moderate Resolution Imaging Spectrora-

¹²⁸ diometer) and VIIRS (Visible Infrared Imaging Radiometer Suite) from global NPP estimates
¹²⁹ (<http://sites.science.oregonstate.edu/ocean.productivity>).

¹³⁰ 2.1 ADCP data and Backscatter estimation

¹³¹ The ADCPs were deployed on the continental slope off the Indian west coast (Fig. 1). Initially a
¹³² set of three ADCPs, it was gradually extended to four more sites to cover the entire EAS basin
¹³³ from Okha (22.26°N) in north to Kanyakumari (6.96 °N) in south. The other two ADCPs are
¹³⁴ Jaigarh at central EAS (CEAS) and Udupi in the transition zone between CEAS & SEAS. The
¹³⁵ extended moorings were deployed in October 2017, except for Kanyakumari which was deployed
¹³⁶ earlier as well but it wasn't included in earlier backscatter study. The moorings are serviced on
¹³⁷ yearly basis usually during October-November or in winter monsoon months. The ADCPs are of
¹³⁸ RD Instruments make, upward-looking and operate at 153.3 kHz. While utmost care is taken to
¹³⁹ position the instrument at ~ 200 m depth, yet for some deployments it's shallow or deeper owing
¹⁴⁰ to drift caused by floater buoyancy - anchor weight balance. Data was collected at hourly interval
¹⁴¹ and the bin size was set to 4 m. The echoes at surface to 10 % range (20 m) means the data at
¹⁴² these is rendered useless and is discarded from further use.

¹⁴³ The procedure followed in processing of the ADCP data are described in [Amol et al., 2014]
¹⁴⁴ and [Mukherjee et al., 2014]. An addition to their methodology was to do depth correction to ac-
¹⁴⁵ commodate the vertical movement of ADCP buoys [Chaudhuri et al., 2020, Mukhopadhyay et al.,
¹⁴⁶ 2020] using data from pressure sensor mounted on the instrument. We have followed the method-
¹⁴⁷ ology laid down in [Aparna et al., 2022] to derive the backscatter time series from ADCP echo
¹⁴⁸ intensity data which is discussed later paragraph. The gaps are filled using the grafting method of
¹⁴⁹ [Mukhopadhyay et al., 2020] once the zooplankton biomass time series is constructed.

150 The primary objective of ADCP usage is to obtain vertical current profile at a point location. It
151 is achieved by using the echo intensity received at the ADCP transducer. The instrument sensors
152 doesn't directly give backscatter, as echo intensity is range independent. Range correction has to
153 be performed before echo intensity (E) is converted to Backscatter (B). Received signal strength
154 indicator (RSSI), also called the conversion factor (Kc) which is specific to a sensor is used along with
155 the corresponding reference echo intensity (Er). It's important to state that for the same device Kc
156 remains unchanged while Er varies over each subsequent deployment. The backscattering strength
157 (in dB) is given by [Mullison, 2017]:

$$158 \quad B = [C - L_{DBM} - P_{DBW}] + 2\alpha R + 10\log_{10}[(T_{TD} + 273.16)R^2] + 10\log_{10}[10^{K_c(E-E_r)/10} - 1]$$

159 where C is an empirical constant, L_{DBM} is $10\log_{10}L$ where L is the transmit pulse length in
160 meters, P_{DBW} is $10\log_{10}P$ (P is transmitted power in watts), α is the sound absorption coefficient
161 of water (in $dB m^{-1}$), T_{TD} is the temperature (in ${}^\circ C$) at the depth of positioned instrument, R
162 is the slant range (in meters) from transducer to the scatterers and E_r is the reference level of E
163 taken in real-time (unit counts). E_r in our case is taken from first (last) measured profile when the
164 instrument is in air before (after) deployment (retrieval). The backscattering strength is referenced
165 to $(4\pi m^{-1})$ [Deines, 1999, Mullison, 2017]. Aparna et al. [2022] has discussed the relevance of each
166 of the term to the total backscattering strength. Our analysis also suggests that the α does not
167 affect the final results.

168 2.2 Zooplankton data and estimation of biomass

169 The zooplankton samples were collected in the vicinity (~ 10 km) of ADCP mooring site twice; once
170 prior retrieval and again post deployment of moorings so that there is overlap in the ADCP time
171 instance and in situ zooplankton samples. The sampling is done at the mooring location during

¹⁷² servicing cruises on board RV Sindhu Sankalp and RV Sindhu Sadhana (Table 2). Multi-plankton
¹⁷³ net (MPN) (100 μm mesh size, 0.5 m^2 mouth area) was used to get samples in the pre-determined
¹⁷⁴ depth ranges; water volume filtered was calculated by the product of sampling depth range and the
¹⁷⁵ mouth area of net. The depth range and timing of sample collection was different throughout the
¹⁷⁶ MPN hauls (refer [Table 2](#)). From 2020 onward, the depth-range was standardized to the bins of 0
¹⁷⁷ - 25, 25 - 50, 50 - 75, 75 - 100, 100 - 150 (units are in meters). The collected zooplankton samples
¹⁷⁸ were then preserved in 5 % formaldehyde solution until it's transferred to laboratory. To measure
¹⁷⁹ zooplankton wet weight accurately, the gelatinous forms/salps were separated. [[Aparna et al.,](#)
¹⁸⁰ [2022](#)] had reported the calanoid copepods, cyclopoid copepods, Poecilostomatoida, Harpacticoida,
¹⁸¹ appendicularians, euphausids, ostracods, and chaetognaths as the major groups of zooplanktons
¹⁸² contributing to the biomass of net samples from the mooring sites. The backscatter obtained earlier
¹⁸³ is averaged in vertical corresponding to the specific MPN hauls for each site. The backscatter is
¹⁸⁴ linear regressed with respective biomass to establish their relationship, which has been demonstrated
¹⁸⁵ in numerous previous studies [[Flagg and Smith, 1989](#), [Heywood et al., 1991](#), [Jiang et al., 2007](#),
¹⁸⁶ [Aparna et al., 2022](#)].

¹⁸⁷ We calculated the regression equation to be $y = 0.0203 x + 4.01$ and, which is well within the
¹⁸⁸ error range of the regression equation of [[Aparna et al., 2022](#)], $y = (0.02 \pm 0.004) x + (4.14 \pm 0.36)$
¹⁸⁹ with a correlation of 0.53 ([Fig. 2](#)). The correlation value in our case is 0.54; the minor difference is
¹⁹⁰ due to higher number of data points (159) in the present study.

¹⁹¹ **2.3 Biomass time series and estimation of standing stock**

¹⁹² The zooplankton biomass time series ([Fig. 3](#)) is created from the above derived linear relationship:
¹⁹³ $\log_{10}(\text{biomass}) = m * \text{Backscatter} + k$, where m is slope and k is intercept. The time series shows

194 the pattern of diel vertical migration (DVM) at all the mooring sites during dawn (\sim 0600-0700
195 hours) and dusk (\sim 1800-1900 hours). It is evident in earlier studies using backscatter [Ashjian
196 et al., 2002, Smith and Madhupratap, 2005, Inoue et al., 2016, Ursella et al., 2018] and in situ
197 zooplankton data [Padmavati et al., 1998]. The implication of DVM is a higher biomass at surface
198 during the night as zooplankton feeds and a lower biomass at daytime as they descend to subsurface
199 depths. The overall biomass over the time period of a day may vary but the DVM doesn't affect
200 the seasonal variation as shown by ([Jiang et al., 2007, Aparna et al., 2022]). Since our goal is to
201 study the seasonal variation, delineating the daily biomass is sufficient. The biomass time series
202 and seasonal cycle is discussed in subsection 4.1.

203 The standing stock is determined by taking the depth integral of biomass over the water column.
204 To maintain the consistency of standing stock estimation, only those deployments that doesn't lack
205 data at any depth in the entire range of 24 - 120 m are considered for analysis. The lack of data in
206 the above mentioned depth range is due to deviation in positioning of ADCP sensor in the water
207 column. A swift alteration in bathymetry along the continental slope implies that the mooring
208 might anchor at a different depth than planned, hence a change in the predicted position of ADCP.
209 This leads to gap in data at few mooring sites for some year. For example, for the northern-most
210 mooring at Okha, data is not available for the entire upper 120 m depth for the second deployment.
211 Also at Jaigarh, where the surface to \sim 60m data (in 3rd deployment) and Kollam, where 80 m
212 and below (in 4th deployment) is unavailable and hence discarded from standing stock estimation.
213 There are few deployments where no data or bad data was recorded e.g, at Udupi (4th deployment)
214 and Kanyakumari (6th deployment). The seasonal cycle of standing stock for 24 - 120 m available
215 data is explored in subsection 4.2.

216 **2.4 Mixed-layer depth, temperature and oxygen**

217 As we are using a 153.3 kHz ADCP moored at \sim 150 m, the top \sim 10% of data is unusable
218 because of surface echoes. MLD in EAS is of the order \sim 20 to 40 m during summer monsoon
219 [Shetye et al., 1990, Sreenivas et al., 2008] especially in the SEAS. Although it is possible to use
220 the near surface ADCP data after due noise correction; it is beyond the scope of present study.
221 The temperature data is used from [Chatterjee et al., 2012] which is a monthly climatology having
222 1° spatial resolution. Monthly climatology of oxygen data is obtained from World Ocean Atlas
223 2013 [García et al., 2014] which contains objectively analyzed 1° climatological fields of in situ
224 measurements.

225 **2.5 Chlorophyll and net primary productivity data**

226 Previous study based on ADCP data of EAS [Aparna et al., 2022] have used SeaWiFS based chloro-
227 phyll data for comparison with climatology of zooplankton standing stock (ZSS). The SeaWiFS was
228 at its end of service in 2010, hence we use new chlorophyll product. The present study has been
229 conducted using Global Ocean Colour, biogeochemical, L3 data obtained from the [E.U. Copernicus](#)
230 [Marine Service Information](#). The daily data is available at a spatial resolution of 4 km.

231 While chlorophyll is used to compare with the variation in climatology of zooplankton standing;
232 the growth efficiencies of zooplankton are directly linked to primary production levels, emphasizing
233 the interconnectedness between primary producers and consumers in marine food webs [?]. In
234 their study, [Aparna et al., 2022] has emphasized on the collapse of the predator-prey relationship
235 between zooplankton-phytoplankton using climatological data. We showcase their interdependency
236 or the lack thereof using net primary productivity models. Moderate Resolution Imaging Spectro-
237 radiometer (MODIS) based net primary productivity (NPP) data at a resolution of $0.16^{\circ} \times 0.16^{\circ}$

238 was obtained from Oregon State University. They have employed three different schemes to obtain
239 NPP from Chlorophyll concentration. Those are discussed below in brief. The first is Vertically
240 Generalized Production Model (VGPM). The NPP (a rate term) is to be derived from chlorophyll
241 (a standing stock) using chlorophyll-specific assimilation efficiency for carbon fixation. The single
242 biggest unknown in all models based on chlorophyll is how this rate term is described. VGPM
243 considers the primary productivity to be dependent on day length and maximum daily NPP within
244 a water column. The second is Carbon-based Productivity Model (CbPM) which NPP to phy-
245toplankton carbon biomass and growth rate. The third is Carbon, Absorption, and Fluorescence
246 Euphotic-resolving (CAFE) mode; first described by [Silsbe et al., 2016] takes various other factors
247 into NPP calculations. We explore these NPP models and try to explain the variation in ZSS.

248 3 Climatology of zooplankton biomass and standing stock

249 The previous study of zooplankton in EAS based on ADCP backscatter was consisting of three
250 sites: Mumbai in NEAS, Goa in CEAS and Kollam in SEAS. The extended mooring sites are at
251 Okha at NEAS, Jaigarh at CEAS, Udupi in the transition zone of CEAS & SEAS and Kanyakumari
252 at SEAS is the southern most location in our study area.

253 ADCP data from three mooring sites were analysed from 2012 to 2020 in [Aparna et al., 2022].
254 They have fine-tuned the methodology to obtain backscatter and estimated zooplankton biomass
255 from it using in situ volumetric zooplankton biomass data. A comparison is made in later para-
256 graphs, since the methodology remains same in the current study and new time series data is
257 available. The monthly climatology of biomass and ZSS is computed for all locations having valid
258 data in 24 - 140 m depth range ([Fig. 4](#)).

259 The high biomass regime in the upper ocean and low biomass regime in deeper depths is differ-

260 entiated using a biomass contour: 215 mg m^{-3} off Mumbai, Goa, Kollam, Jaigarh and Udupi; 175
261 mg m^{-3} off Okha and Kanyakumari. For simplicity, this biomass contour is abbreviated to be z215
262 & z175 and its depth is denoted as D215 & D175, respectively. The choice of biomass contour isn't
263 abrupt; firstly, it is carefully chosen to accommodate the seasonal variation, as a shift to biomass
264 contour lower than the z215 would be unviable as our data is only till 140 m depth, for example in
265 the case of Kollam, the D215 exceeds 140 during few months of 2022 ([Fig. 3](#)). A higher biomass
266 contour would lead to inferior view of the seasonal cycle as in the case of Kanyakumari and Okha
267 where 215 mg m^{-3} biomass contour is often low enough to reach $\sim 20 - 30$ m depths, hence z175 is
268 chosen here. Secondly, it allows us to link the seasonal variation of biomass to the physico-chemical
269 properties.

270 The climatology of zooplankton biomass and ZSS ([Fig. 4](#)) is discussed at locations northward
271 starting from southernmost mooring site off Kanyakumari.

272 3.1 Southern EAS

273 During mid-march off Kanyakumari, the depth of 23° C isotherm (henceforth D23) shallows along-
274 with oxycline (marked by 2.1 ml L^{-1}) and a rise in biomass is observed ([Fig. 4 g1](#)). The z175
275 is shallower from May onward to October and the zooplankton biomass is comparatively higher
276 than rest of the year. The D175 deepens starting from October and the relatively high biomass in
277 water column is maintained till late December. However, this increase in D175 isn't reflected as
278 an increase in ZSS because of low biomass in the entire water column. A gradual increase is seen
279 in the chlorophyll biomass starting from April and the peak is attained in June ([Fig. 4 g2](#)). The
280 ZSS is increased in June, however the growth is minimal. There is almost no seasonal variation
281 in ZSS off Kanyakumari (seasonal ZSS range, 2.67 gm m^{-2}) as compared to the ZSS variation at

²⁸² the nearest northern mooring site off Kollam (seasonal ZSS range, 4.86 gm m^{-2}), where a strong
²⁸³ seasonal cycle is observed and the D215 is deeper for any given month.

²⁸⁴ Off Kollam, a higher biomass is present in the larger portion of water column and the D215 is
²⁸⁵ at $\sim 110 \text{ m}$ during Mar-May ([Fig. 4 f1](#)). Similar to z175 off Kanyakumari, the decrease in biomass
²⁸⁶ with depth is subtle below z215. Starting from March, the D215 begins to shallow with progress
²⁸⁷ in time till August. During this period, a sharp decrease is seen in the D23 ($\sim 80 \text{ m}$ in June
²⁸⁸ to September) while the oxycline (1.7 ml L^{-1}) overshoots the thermocline ([Fig. 4 f1](#)). A steep
²⁸⁹ rise in chlorophyll biomass is seen off Kollam and its peak is attained in August ([Fig. 4 f2](#)). The
²⁹⁰ ZSS declines in the same period and reaches a minimum when the chlorophyll biomass is at its
²⁹¹ peak. The chlorophyll biomass decreases rapidly in the following months, while the ZSS increases
²⁹² and a maximum is seen during October. This feature was earlier reported by [[Aparna et al., 2022](#)]
²⁹³ showing disproportionate interaction between zooplankton and phytoplankton. It begs the question
²⁹⁴ about existing understanding of predator - prey relationship in a regional-scale ecological system.
²⁹⁵ A similar feature is seen further north, off Udupi which sits at the transition zone of SEAS &
²⁹⁶ CEAS, albeit with a relatively weaker zooplankton biomass. The peak of chlorophyll and minimum
²⁹⁷ of ZSS occurs in September ([Fig. 4 e2](#)) which is one month later than off Kollam. The 2.1 ml L^{-1}
²⁹⁸ oxygen contour overshoots thermocline, however it reaches to a much shallow depth of $\sim 20 \text{ m}$
²⁹⁹ during July to October unlike any other location in our EAS study area. The D215 vaguely follows
³⁰⁰ D23; with the gradual shallowing from March onward reaching $\sim 60 \text{ m}$ in September and a steep
³⁰¹ decline afterwards till November ([Fig. 4 e1](#)). The decrease of biomass with depth is moderate in
³⁰² comparison to Kollam.

303 **3.2 Central EAS**

304 Off Goa, the D215 seasonal trend is similar to Udupi and is entirely restricted by D23 & 1.7 ml L^{-1}
305 oxygen contour that closely follows it. During March-May, the D215 is at $\sim 80 - 100 \text{ m}$ which
306 shallows with onset of summer monsoon ([Fig. 4 d1](#)); the chlorophyll biomass increases during this
307 period and the maximum occurs in August after which the chlorophyll biomass and ZSS ([Fig. 5](#))
308 both decrease in September. Although we witness an increase in chlorophyll biomass in October,
309 the D215 is restricted to the $\sim 50 \text{ m}$ in this period and the ZSS is at its minimum similar to what
310 is observed off Udupi (Kollam) during September (August). The ZSS rapidly increases and reaches
311 its maximum in January, sustained till March and then gradually declines. Unlike the previous
312 locations, the biomass off Goa decreases rapidly below the z215 as reported earlier [[Aparna et al.](#),
313 [2022](#)], reaching as low as 60 mg m^{-3} at 130 m during June to September ([Fig. 4 d1](#)).

314 The ZSS off Jaigarh is identical but stronger to that of off Goa, owing to an higher biomass above
315 z215 and the comparatively deeper D215 ([Fig. 4 c1](#)). The D215 follows D23 & oxycline for most
316 of the year and it only exceeds during October-December. From the ZSS maximum in February
317 ([Fig. 4 c2](#)), it steadily decreases and attains a minimum in September (coincides with lower D200),
318 a rapid rise is seen in the following months. What's intriguing is a presence of strong seasonal cycle
319 in ZSS off Jaigarh (10.38 gm m^{-2} , highest among all locations) although the seasonal variation in
320 chlorophyll biomass ([Fig. 4 c2](#)) is visibly non-existent (0.15 mg m^{-3} , lowest among all locations).
321 This is an exact opposite scenario of Kanyakumari site, where an insignificant seasonal variation in
322 ZSS (2.67 gm m^{-2}) is seen even though the chlorophyll biomass varies strongly (1.62 mg m^{-3}).

323 Starting from Kollam ([Fig. 4 f1](#)) and moving northward to Jaigarh ([Fig. 4 c1](#)), we see that the
324 core of high zooplankton biomass gradually shifts from summer monsoon (off Kollam) to winter
325 monsoon (off Jaigarh), with the transition of upper ocean zooplankton biomass happening along

326 Udupi and Goa. On the contrary, the chlorophyll biomass tends to have low seasonal range as we
327 move northward from SEAS, with Jaigarh having the least seasonal variation.

328 **3.3 Northern EAS**

329 Further north of Jaigarh, off Mumbai the D215 follows a similar pattern i.e, a deeper D215 in
330 December to early April, resulting in a higher ZSS in the same period ([Fig. 4 b2](#)). The D23 off
331 Mumbai follows D215 and the oxycline follows an erratic pattern, reaching depths > 140 during
332 January to March ([Fig. 4 b1](#)); when a higher biomass is observed above z215. The chlorophyll
333 biomass shows seasonal variation albeit lower than the SEAS counterpart. Its peak occurs in
334 August, then decreases rapidly and increases from October onward maintaining the biomass at 0.5
335 $mg\ m^{-3}$ till March. In zooplankton biomass climatology, during September-October a thin layer
336 of low biomass regime is seen at depths \sim 30 - 40 m, combined with shallow D215 resulting in a
337 ZSS minimum. The ZSS increases rapidly from its minima in October in the following month as
338 the D215 deepens and the maximum occurs in February. The chlorophyll biomass decreases from
339 March and a gradual decrease in ZSS is seen till July, after which the ZSS basically flattens even
340 though the chlorophyll increases.

341 At the northernmost site of EAS i.e, off Okha, a noticeable feature is a much higher oxygen in
342 upper ocean except during summer monsoon. The biomass above z200 is much weaker ([Fig. 4 a1](#))
343 compared to Mumbai as seen in the zooplankton biomass climatology which leads to a relatively
344 lower ZSS ([Fig. 4 a2](#)). The D200 shallows from February (coinciding with ZSS maximum) to it's
345 minimum in August, remains visibly flat till September and then increases steadily till December
346 and rapidly afterwards. There's two chlorophyll peak off Okha; one in February [[Keerthi et al., 2017](#)]
347 and the other during August in summer monsoon [[Lévy et al., 2007](#)]. The ZSS remains flat

348 in summer monsoon period i.e, June to September, although the chlorophyll biomass increases in
349 this time. Afterwards, ZSS gradually increases and attains its maximum in February same as the
350 chlorophyll biomass. The ZSS sustains this maximum till March, declines rapidly in April and then
351 gradually till July.

352 **3.4 Comparison to previous result**

353 A comparison with the zooplankton biomass and standing stock climatology of previous work
354 [Aparna et al., 2022] is made in this section for the locations of Mumbai, Goa and Kollam. In the
355 previous study data from 2012 to 2020 is used, while the present study includes data from 2017 to
356 2023.

357 It is observed that D215 is shallower at all locations and as a result a lower ZSS is seen in the
358 climatology of the present study (Fig. 5). The difference in D215 is prominent off Goa; while in the
359 previous climatology (Fig. 5 b1) the D215 is deeper and lies along D23, in the present climatological
360 data (Fig. 5 b2) the D215 is shallower and lies \sim 20 - 40 m above the D23 during January to April.
361 A relatively lower biomass is present above z215 year round which reflects in overall lower ZSS. This
362 goes same for the biomass off Mumbai (Fig. 5 a1 & a2) i.e, a comparatively shallow D215 and lower
363 ZSS in comparison with [Aparna et al., 2022]. Instead of a ZSS maxima in February, in the present
364 data, the maxima is sustained in march, which could be due to the lower value of ZSS in February.
365 The second maxima occurs in August (Fig. 5 d1) which is less pronounced in present study (Fig. 5
366 d2). Similar to Goa, there is dramatic decrease in the minima that occurs in October and ZSS
367 increases rapidly post October till February. Off Kollam, a higher biomass is observed from May to
368 June in previous study, while in the present study, along with May to June, a higher biomass is seen
369 from September to November (Fig. 4 c2) which is reflected as a minima of ZSS occurring in August

370 (Fig. 4 d2). The higher ZSS on either side to this minima is less pronounced in previous data. This
371 difference in ZSS is clearly seen in the correlation, which is 0.60 off Kollam, while it is 0.94 and 0.98
372 off Mumbai and Goa, respectively. Note that the correlation only shows how similar the ZSS trend
373 is and doesn't tell us about the deviation in magnitude in present study. Chlorophyll biomass shows
374 stronger peak for all locations in August in present study, when the zooplankton-phytoplankton
375 relationship discrepancy is observed off Kollam similar to results reported in previous climatology.

376 4 The seasonal cycle and variability

377 In the following section we will describe the zooplankton biomass time series followed by a discussion
378 on the seasonal cycle.

379 Biomass contour to demarcate upper (high biomass) to lower (low biomass) regimes is devised
380 for each zooplankton time series to show their seasonality. A preliminary analysis of the biomass
381 time series in daily and monthly averaged scale shows that the biomass decreases with increasing
382 depth (Fig. 3) at all the seven locations. The rate of biomass decrease with depth, roughly defined
383 as the difference between the mean biomass at 40 m and 104 m depth, is highest off Jaigarh and
384 Mumbai as it has higher biomass in upper ocean (Fig. 6 c,b). This is followed by CEAS locations
385 Goa and Udupi (Fig. 6 d,e). While the biomass decrease with depth is lower off Kollam from
386 2017 to 2020, it becomes considerably high from thereon (Fig. 6 f). The rate of decrease is lowest
387 off Kanyakumari. Following is the order of their decrease rate of biomass: Jaigarh (96 mg m^{-3}),
388 Mumbai (91 mg m^{-3}), Okha (79 mg m^{-3}), Udupi (78 mg m^{-3}), Kollam(73 mg m^{-3}), Goa (72 mg m^{-3}) and Kanyakumari (39 mg m^{-3}). The mean and standard deviation is shown in Table 3.
389 Following poleward along the slope, the mean biomass at 40 m off Kanyakumari is the least \sim
390 207 mg m^{-3} which increases drastically to 272 mg m^{-3} off Kollam. It decreases till Goa and

then increases to a maximum of 278 mg m^{-3} off Jaigarh. Off Mumbai the mean biomass is 272 mg m^{-3} , and further north off Okha, it declines to 230 mg m^{-3} . A similar trend is observed in mean biomass at 104 m depth of all locations and their corresponding standard deviation. A pattern that develops from this is observed, with lower mean biomass off Okha (northernmost of EAS) and off Goa (CEAS) bifurcated by higher mean biomass off Mumbai & Jaigarh; while the lower mean biomass off Udupi (CEAS) and off Kanyakumari (Southernmost of EAS) is divided by higher mean biomass off Kollam. Similarly, from standard deviation of biomass it is inferred that the sites with higher biomass tends to have higher variation over time as in the case of Mumbai, Jaigarh and Kollam.

A comparatively weaker decline in zooplankton biomass with respect to depth off Okha ([Fig. 3 a1,a2](#)) at NEAS is agreeing with earlier reported data [Madhupratap et al. \[2001\]](#), [Smith and Madhupratap \[2005\]](#), [Wishner et al. \[1998\]](#) where oxygen deficit is thought to be the cause, particularly during summer monsoon seen in [\[García et al., 2014\]](#) climatology (figure not shown). The sites at SEAS, especially off Kanyakumari and 2017 to 2020 off Kollam also have weaker decrease [\[Madhupratap et al., 2001\]](#), [\[Aparna et al., 2022\]](#). However, post 2020 the decline in biomass with depth off Kollam is similar to that off Mumbai in stark contrast to its previous years owing to a strong bloom in these years. This growth is reflected as an increase in biomass in the entire water column([Fig. 3 f1,f2](#)) and deepening of D215. Analyzing the demarcating biomass contours (z175, z215 of respective locations) we see a strong seasonality at NEAS, CEAS and SEAS (excluding Kanyakumari). Although a shallow and seasonally invariant D215 is seen for Goa and Kollam during January 2019 to December 2020. While the z175 and z215 is deeper in winter monsoon throughout EAS, at the NEAS regime, the upper ocean shows considerably high biomass during this period as in the case of Okha, Mumbai and Jaigarh. On the contrary, at SEAS regime the upper ocean shows higher

415 biomass during summer monsoon as seen off Udupi, Kollam and Kanyakumari even though the
416 z215 & z175 is shallower in this period.

417 **4.1 Seasonal cycle of biomass**

418 Although the variation in zooplankton biomass time series is inferred from the standard deviation
419 at 40 & 104 m depth, it provides no information about the seasonal cycle. The evaluation is made
420 from performing wavelet analysis on the time series. In the investigation of dominant periods, it is
421 valid to compare the wavelet power (or variability) along a particular period across the time series,
422 but a cross-period wavelet power comparison is not possible [Maraun and Kurths, 2004, Chaudhuri
423 et al., 2020]. It is due to the normalization process which stresses more on the wavelet power of
424 higher period, and hence for the same wavelet power a lower period would have higher variability
425 compared to a higher period.

426 **4.1.1 The annual cycle**

427 The time series has loss of data due to instrument fault or improper position of ADCP in the
428 water column. For example, off Okha during it occurred in the second deployment (Dec-2019 to
429 Dec-2020), the instrument was way below from it's intended depth of 150 m leading to no data in
430 top 140 m water column. It is not possible to construct a continuous record and hence it makes
431 it difficult to interpret the annual cycle where ever the data record is short. So, for 40 m biomass
432 time series we restrict our description to all locations except Okha and Jaigarh while performing
433 wavelet analysis.

434 Off Mumbai, a strong annual cycle (~ 365 days) dominates the seasonal cycle throughout the
435 time series (Fig. 7 b). Annual cycle is comparatively weak off Goa (CEAS) contrary to results of

436 [Aparna et al., 2022] which could be due to shorter time record and low biomass in the recent years.
437 The annual cycle off Udupi & Kollam (SEAS) is strong, however it varies in time and off Kollam
438 the wavelet power is stronger post 2020 ([Fig. 7 f](#)). Further south, off Kanyakumari, the annual
439 cycle weakens having power similar to that of Goa.

440 At 104 m, the annual cycle strengthens off Mumbai and Goa ([Fig. 8 b, d](#)) compared to the
441 annual cycle at 40 m; implying that the biomass seasonal variation at 104 m is robust even though
442 the mean biomass is considerably lower. Annual cycle weakens off Kollam ([Fig. 8 f](#)), although only
443 vague interpretation can be made as it lies beyond the cone of influence.

444 4.1.2 The semi-annual cycle

445 Along with the annual cycle, we observe presence of semi-annual (~ 180 days) cycle at most locations
446 and together they constitute the seasonal cycle. At 40m depth Off Okha the semi-annual period is
447 weak. Off Mumbai however, the semi-annual cycle is present throughout the record and becomes
448 stronger in 2022-2023 ([Fig. 7 b](#)) but not as much as the annual cycle. At Goa we see that the
449 semi-annual period dominates seasonal cycle in the same duration ([Fig. 7 d](#)). The dominance
450 of semi-annual cycle is also seen off Kollam. Although the dominance of semi-annual period in
451 seasonal cycle is seen only for some years, a similar feature was discussed for WICC [[Chaudhuri](#)
452 et al., 2020] where the intra-annual component dominates the seasonal cycle as we go equatorward
453 with a change in the strength of intra-annual component in time. However, off Kanyakumari the
454 semi-annual cycle is absent([Fig. 7 g](#)).

455 Unlike the annual band which becomes stronger at 104 m, the semi-annual band weakens off
456 Mumbai & Goa at the same depth ([Fig. 8 b,d](#)). While the semi-annual band at 104 m becomes
457 relatively stronger compared to the semi-annual band at 40 m off Okha ([Fig. 8 a](#)), it is almost

458 non-existent off Kanyakumari ([Fig. 8 g](#)). The wavelet power of semi-annual cycle is same at 40 m &
459 104 m off Mumbai, Goa and Kollam for most of the data record, but weakens at 104 m compared to
460 40 m during 2022. Investigating the longer time series off Mumbai, Goa and Kollam, it is observed
461 that the semi-annual cycle is comparable to the annual cycle at some instances such as in 2022 and
462 the its strength increases as we move equatorward.

463 4.2 Seasonal cycle of standing stock

464 The zooplankton standing stock time series is obtained by integrating the biomass over 24 - 120
465 m of water column (update figure to include Chl time series, [Fig. 9](#)). The presence of significant
466 variation in the 30-day running mean with recurring burst is seen in the daily data. In NEAS
467 regime, the ZSS maximum occurs during January to late March and early April as seen off Okha,
468 Mumbai, Jaigarh and Goa. However, the decline of ZSS post the maxima is comparatively gradual
469 off Goa which was also visible in the climatology of ZSS ([Fig. 4 d2](#)). The growth in ZSS at NEAS
470 sites during summer monsoon is much lower compared to the SEAS. For example, off Kollam, we
471 observe the presence of double peak, one during May to July and the another during September to
472 November. Similar feature is seen off Udupi, the nearest northern site of Kollam, but with a much
473 higher ZSS during September to November as compared with May to July ZSS. Off Kanyakumari,
474 although there seems to be intra-annual variations, a clear annual cycle is not observed.

475 4.2.1 The annual cycle

476 The absence of annual cycle off Kanyakumari is confirmed with wavelet analysis ([Fig. 9 g1](#)). Off
477 Kollam, the presence of a weak annual cycle is seen contrary to a strong annual cycle of Udupi,
478 however a longer data record is needed as the annual period lies beyond the cone of influence. Off

⁴⁷⁹ Goa ([Fig. 9 d1](#)), the annual cycle was weak for 2018 to early 2020, which strengthened afterwards.
⁴⁸⁰ The annual cycle is strongest off Mumbai ([Fig. 9 b1](#)) throughout the data record and the wavelet
⁴⁸¹ power is highest among all locations as confirmed with Fourier analysis. This analysis reveals the
⁴⁸² presence of strong annual cycle off Jaigarh and Okha at NEAS.

⁴⁸³ 4.2.2 The semi-annual cycle

⁴⁸⁴ Although we observed the absence of annual cycle off Kanyakumari, the wavelet analysis shows
⁴⁸⁵ presence of a semi-annual cycle from early 2019 to late 2021([Fig. 9 g1](#)). This semi-annual feature is
⁴⁸⁶ seen off Kollam ([Fig. 9 f1](#)) with moderate power and with a much higher power off Udupi ([Fig. 9 21](#))
⁴⁸⁷ during 2018 to 2020. Much like the annual cycle off Goa, it's semi-annual period is weak to nearly
⁴⁸⁸ non existent before 2020 and gets strengthened afterwards. Off Mumbai, the semiannual period
⁴⁸⁹ is present from late 2018 to late 2020 and from 2022 onward. Fourier analysis shows that the
⁴⁹⁰ semi-annual cycle off Udupi is comparable to its counterpart off Mumbai during the same period.

⁴⁹¹ The higher beta (β) coefficients off Jaigarh and Kollam implies a significant contribution of low
⁴⁹² frequency variability (higher period) is more compared to the high frequency variability. In fact,
⁴⁹³ a biennial peak is seen off Kollam in the Fourier analysis even with a 3 year record agreeing with
⁴⁹⁴ earlier findings of [Aparna et al. \[2022\]](#), i.e, Kollam having a weak (strong) annual (biennial) cycle.

⁴⁹⁵ 4.3 Annual, intra-annual and intraseasonal variability

⁴⁹⁶ The biomass at a given instance is decomposed to several exclusive period bands spanning days to
⁴⁹⁷ months. DVM is the simplest variation (low period or high frequency) among many that determines
⁴⁹⁸ zooplankton biomass at a given depth, with higher (lower) biomass during night (day) at the surface
⁴⁹⁹ regime for a number of species. Our focus, however is on the variability occurring in the higher

500 period (lower frequency) bands namely, annual, intra-annual and intraseasonal variability. 2019
501 **off Kollam, figure can be added to explain it better**

502 To capture the annual variability, the biomass is filtered with lanczos filter within period of 300 to
503 400 days. The annual variability shows that the contribution of this band to the time series of total
504 biomass is very weak. The annual variability off Kanyakumari (standard deviation 3.64 mg m^{-3})
505 and Okha (3.73 mg m^{-3}) is low, while it is stronger at rest of the basin, with strongest variability off
506 Jaigarh (9.05 mg m^{-3}). **add explanation, Upward phase propagation is observed off Goa**
507 **and it's southern mooring sites.** Similar to the ocean currents [Amol et al., 2014, Chaudhuri
508 et al., 2020], the annual filtered biomass decreases more with depth off Kollam than off Mumbai
509 and the three CEAS sites. **include wavelet coherence results at 40 m of adjacent sites.**

510 The variability at intra-annual (100 - 250 days) band tends to be stronger compared to the
511 annual variability and is strengthened during August to November (Fig. 12) as seen during 2018,
512 2019 and 2022. Intra-annual variability increases as we move equatorward with higher variability
513 seen off Goa, Udupi and Kollam, although off Kanyakumari the variability is diminished. However,
514 Fourier analysis of the daily biomass time series suggests presence of signals within the intra-annual
515 band off Kanyakumari, e.g, power peaks at ~ 140 and ~ 220 days implying that the variability is
516 strictly restricted to narrow bands within intra-annual band. There is a significant variation in the
517 strength of intra-annual variability (Fig. 12) and its component (Fig. 7) with time. For example, off
518 Goa at 40 m during August to November of 2020 and 2022, the intra-annual component is weak and
519 strong, respectively (Fig. 12). This difference is due to the spread of energy among all intra-annual
520 periods for 2022, while during 2020 the wavelet energy is only present in the semi-annual periods,
521 resulting in a overall weaker intra-annual component.

522 The intraseasonal band, defined as the variability occurring between periods of few days to 90

523 days is split into two categories; a high-frequency part (period < 30 days) and a low-frequency
524 part (30 < period < 90 days. The presence of low-frequency intraseasonal signals is observed in
525 the wavelet analysis of biomass at 40 m ([Fig. 7](#)) and 104 m ([Fig. 8](#)) as bursts during few months
526 distinctive to each mooring location. The wavelet power at 40 m in low-frequency intraseasonal
527 band peaks during September to December off Mumbai, Jaigarh and Kanyakumari while no such
528 general observation is found in other locations. However, the wavelet power at 104 m in comparison
529 to 40 m suggests a decrease in its strength at respective locations. Lanczos filtered biomass in 30 to
530 90 day period shows that the intraseasonal variability is strong during August to November off all
531 location ([Fig. 11](#)). This is in contrast to the WICC intraseasonal band which is strong during winter
532 monsoon [Amol et al., 2014, Chaudhuri et al., 2020]. The low frequency intraseasonal variability
533 is higher in the upper ocean, however it can extend to deeper depths (~ 140) for some years e.g,
534 off Kollam during 2022 ([Fig. 11 f](#)). The magnitude of low-frequency intraseasonal component is
535 high as we move equatorward till Kollam and declines off Kanyakumari ([Fig. 11 g](#)). As noted
536 earlier in variability of the intra-annual component, the intra-seasonal component's strength and
537 its variability is transient in nature.

538 **4.4 discussion**

539 interannual variability of CHl-a is less significant in comparison to the seasonal variability [Shi and
540 Wang, 2022].

541 \therefore Deviation from climatology, 2019, off Goa, and Kanyakumari. Goa has lower biomass
542 throughout 2019.

543 \therefore the net transport in upper 500 m is 10^{**7} m³/s in easter arabian sea, which flows out of the
544 sea in summer. 10^{**6} in winter monsoon (shi et al. 1999).

545 **References**

546 Anna-Karin Almén and Tobias Tamelander. Temperature-related timing of the spring bloom and match between
547 phytoplankton and zooplankton. *Marine Biology Research*, 16(8-9):674–682, 2020.

548 P Amol, D Shankar, V Fernando, A Mukherjee, SG Aparna, R Fernandes, GS Michael, ST Khalap, NP Satelkar,
549 Y Agarvadekar, et al. Observed intraseasonal and seasonal variability of the west india coastal current on the
550 continental slope. *Journal of Earth System Science*, 123(5):1045–1074, 2014.

551 P Amol, Suchandan Bemal, D Shankar, V Jain, V Thushara, V Vijith, and PN Vinayachandran. Modulation of
552 chlorophyll concentration by downwelling rossby waves during the winter monsoon in the southeastern arabian
553 sea. *Progress in Oceanography*, 186:102365, 2020.

554 SG Aparna, DV Desai, D Shankar, AC Anil, Shrikant Dora, and R Khedekar. Seasonal cycle of zooplankton standing
555 stock inferred from adcp backscatter measurements in the eastern arabian sea. *Progress in Oceanography*, 203:
556 102766, 2022.

557 Carin J Ashjian, Sharon L Smith, Charles N Flagg, and Nasseer Idrisi. Distribution, annual cycle, and vertical
558 migration of acoustically derived biomass in the arabian sea during 1994–1995. *Deep Sea Research Part II:*
559 *Topical Studies in Oceanography*, 49(12):2377–2402, 2002.

560 K Banse and DC English. Geographical differences in seasonality of czcs-derived phytoplankton pigment in the
561 arabian sea for 1978–1986. *Deep Sea Research Part II: Topical Studies in Oceanography*, 47(7-8):1623–1677, 2000.

562 Karl Banse. Hydrography of the arabian sea shelf of india and pakistan and effects on demersal fishes. In *Deep sea*
563 *research and oceanographic Abstracts*, volume 15, pages 45–79. Elsevier, 1968.

564 Karl Banse. Zooplankton: pivotal role in the control of ocean production: I. biomass and production. *ICES Journal*
565 *of marine Science*, 52(3-4):265–277, 1995.

- 566 WE Barraclough, RJ LeBrasseur, and OD Kennedy. Shallow scattering layer in the subarctic pacific ocean: detection
567 by high-frequency echo sounder. *Science*, 166(3905):611–613, 1969.
- 568 H. P. Batchelder, J. R. VanKeuren, R. D. Vaillancourt, and E. Swift. Spatial and temporal distributions of acoustically
569 estimated zooplankton biomass near the marine light-mixed layers station (59°30'n, 21°00'w) in the north atlantic
570 in may 1991. *Journal of Geophysical Research: Oceans*, 100:6549–6563, 1995. doi: 10.1029/94jc00981.
- 571 John C Brock and Charles R McClain. Interannual variability in phytoplankton blooms observed in the northwestern
572 arabian sea during the southwest monsoon. *Journal of Geophysical Research: Oceans*, 97(C1):733–750, 1992.
- 573 John C Brock, Charles R McClain, Mark E Luther, and William W Hay. The phytoplankton bloom in the north-
574 western arabian sea during the southwest monsoon of 1979. *Journal of Geophysical Research: Oceans*, 96(C11):
575 20623–20642, 1991.
- 576 Abhisek Chatterjee, D Shankar, SSC Shenoi, GV Reddy, GS Michael, M Ravichandran, VV Gopalkrishna,
577 EP Rama Rao, TVS Udaya Bhaskar, and VN Sanjeevan. A new atlas of temperature and salinity for the north
578 indian ocean. *Journal of Earth System Science*, 121:559–593, 2012.
- 579 Anya Chaudhuri, D Shankar, SG Aparna, P Amol, V Fernando, A Kankonkar, GS Michael, NP Satelkar, ST Khalap,
580 AP Tari, et al. Observed variability of the west india coastal current on the continental slope from 2009–2018.
581 *Journal of Earth System Science*, 129(1):57, 2020.
- 582 Anya Chaudhuri, P Amol, D Shankar, S Mukhopadhyay, SG Aparna, V Fernando, and A Kankonkar. Observed
583 variability of the west india coastal current on the continental shelf from 2010–2017. *Journal of Earth System
584 Science*, 130:1–21, 2021.
- 585 Boris Cisewski, Volker H Strass, Monika Rhein, and Sören Krägesky. Seasonal variation of diel vertical migration
586 of zooplankton from adcp backscatter time series data in the lazarev sea, antarctica. *Deep Sea Research Part I:
587 Oceanographic Research Papers*, 57(1):78–94, 2010.
- 588 Kent L Deines. Backscatter estimation using broadband acoustic doppler current profilers. In *Proceedings of the
589 IEEE Sixth Working Conference on Current Measurement (Cat. No. 99CH36331)*, pages 249–253. IEEE, 1999.
- 590 A Edvardsen, D Slagstad, KS Tande, and P Jaccard. Assessing zooplankton advection in the barents sea using
591 underway measurements and modelling. *Fisheries Oceanography*, 12(2):61–74, 2003.
- 592 S Fielding, G Griffiths, and HSJ Roe. The biological validation of adcp acoustic backscatter through direct comparison
593 with net samples and model predictions based on acoustic-scattering models. *ICES Journal of Marine Science*,
594 61(2):184–200, 2004.
- 595 Charles N Flagg and Sharon L Smith. On the use of the acoustic doppler current profiler to measure zooplankton
596 abundance. *Deep Sea Research Part A. Oceanographic Research Papers*, 36(3):455–474, 1989.

- 597 H. E. García, R. A. Locarnini, T. P. Boyer, J. I. Antonov, A. V. Mishonov, O. K. Baranova, M. M. Zweng, J. R.
598 Reagan, and D. R. Johnson. Dissolved oxygen, apparent oxygen utilization, and oxygen saturation. *NOAA Atlas*
599 *NESDIS 75*, 3, 2014.
- 600 Charles H Greene, Peter H Wiebe, Chris Pelkie, Mark C Benfield, and Jacqueline M Popp. Three-dimensional
601 acoustic visualization of zooplankton patchiness. *Deep Sea Research Part II: Topical Studies in Oceanography*, 45
602 (7):1201–1217, 1998.
- 603 Charles F Greenlaw. Acoustical estimation of zooplankton populations 1. *Limnology and Oceanography*, 24(2):
604 226–242, 1979.
- 605 Davide Guerra, Katrin Schroeder, Mireno Borghini, Elisa Camatti, Marco Pansera, Anna Schroeder, Stefania
606 Sparnocchia, and Jacopo Chiggiato. Zooplankton diel vertical migration in the corsica channel (north-western
607 mediterranean sea) detected by a moored acoustic doppler current profiler. *Ocean Science*, 15(3):631–649, 2019.
- 608 James M Hamilton, Kate Collins, and Simon J Prinsenberg. Links between ocean properties, ice cover, and plankton
609 dynamics on interannual time scales in the canadian arctic archipelago. *Journal of Geophysical Research: Oceans*,
610 118(10):5625–5639, 2013.
- 611 Graeme C Hays. A review of the adaptive significance and ecosystem consequences of zooplankton diel vertical
612 migrations. In *Migrations and Dispersal of Marine Organisms: Proceedings of the 37 th European Marine Biology*
613 *Symposium held in Reykjavík, Iceland, 5–9 August 2002*, pages 163–170. Springer, 2003.
- 614 PJ Herring, MJR Fasham, AR Weeks, JCP Hemmings, HSJ Roe, PR Pugh, S Holley, NA Crisp, and MV Angel.
615 Across-slope relations between the biological populations, the euphotic zone and the oxygen minimum layer off
616 the coast of oman during the southwest monsoon (august, 1994). *Progress in Oceanography*, 41(1):69–109, 1998.
- 617 Karen J Heywood, S Scrope-Howe, and ED Barton. Estimation of zooplankton abundance from shipborne adcp
618 backscatter. *Deep Sea Research Part A. Oceanographic Research Papers*, 38(6):677–691, 1991.
- 619 Laura Hobbs, Neil S Banas, Jonathan H Cohen, Finlo R Cottier, Jørgen Berge, and Øystein Varpe. A marine
620 zooplankton community vertically structured by light across diel to interannual timescales. *Biology Letters*, 17(2):
621 20200810, 2021.
- 622 Raleigh R Hood, Lynnath E Beckley, and Jerry D Wiggert. Biogeochemical and ecological impacts of boundary
623 currents in the indian ocean. *Progress in Oceanography*, 156:290–325, 2017.
- 624 Ryuichiro Inoue, Minoru Kitamura, and Tetsuichi Fujiki. Diel vertical migration of zooplankton at the s 1 bioge-
625 chemical mooring revealed from acoustic backscattering strength. *Journal of Geophysical Research: Oceans*, 121
626 (2):1031–1050, 2016.
- 627 Songnian Jiang, Tommy D Dickey, Deborah K Steinberg, and Laurence P Madin. Temporal variability of zooplankton
628 biomass from adcp backscatter time series data at the bermuda testbed mooring site. *Deep Sea Research Part I:*
629 *Oceanographic Research Papers*, 54(4):608–636, 2007.

- 630 R Jyothibabu, NV Madhu, H Habeebrehman, KV Jayalakshmy, KKC Nair, and CT Achuthankutty. Re-evaluation
631 of ‘paradox of mesozooplankton’ in the eastern arabian sea based on ship and satellite observations. *Journal of*
632 *Marine Systems*, 81(3):235–251, 2010.
- 633 Myounghee Kang, Sunyoung Oh, Wooseok Oh, Dong-Jin Kang, SungHyun Nam, and Kyounghoon Lee. Acoustic
634 characterization of fish and macroplankton communities in the seychelles-chagos thermocline ridge of the southwest
635 indian ocean. *Deep Sea Research Part II: Topical Studies in Oceanography*, 213:105356, 2024.
- 636 Madhavan Girijkumari Keerthi, Matthieu Lengaigne, Marina Levy, Jerome Vialard, Vallivattathillam Parvathi,
637 Clément de Boyer Montégut, Christian Ethé, Olivier Aumont, Iyyappan Suresh, Valiya Parambil Akhil, et al.
638 Physical control of interannual variations of the winter chlorophyll bloom in the northern arabian sea. *Biogeosciences*,
639 14(15):3615–3632, 2017.
- 640 Punam A Khandagale, Vaibhav D Mhatre, and Sujitha Thomas. Seasonal and spatial variability of zooplankton
641 diversity in north eastern arabian sea along the maharashtra coast. *Journal of the Marine Biological Association*
642 *of India*, 64(1):25–32, 2022.
- 643 Corinne Le Qu, Robbie M Andrew, Josep G Canadell, Stephen Sitch, Jan Ivar Korsbakken, Glen P Peters, Andrew C
644 Manning, Thomas A Boden, Pieter P Tans, Richard A Houghton, et al. Global carbon budget 2016. *Earth System*
645 *Science Data*, 8(2):605–649, 2016.
- 646 Marina Lévy, D Shankar, J-M André, SSC Shenoi, Fabien Durand, and Clément de Boyer Montégut. Basin-wide
647 seasonal evolution of the indian ocean’s phytoplankton blooms. *Journal of Geophysical Research: Oceans*, 112
648 (C12), 2007.
- 649 M Li, A Gargett, and K Denman. What determines seasonal and interannual variability of phytoplankton and
650 zooplankton in strongly estuarine systems? *Estuarine, Coastal and Shelf Science*, 50(4):467–488, 2000.
- 651 Yanliang Liu, Jingsong Guo, Yuhuan Xue, Chalermrat Sangmanee, Huiwu Wang, Chang Zhao, Somkiat Khokiat-
652 tiwong, and Weidong Yu. Seasonal variation in diel vertical migration of zooplankton and micronekton in the
653 andaman sea observed by a moored adcp. *Deep Sea Research Part I: Oceanographic Research Papers*, 179:103663,
654 2022.
- 655 M Madhupratap, P Haridas, Neelam Ramaiah, and CT Achuthankutty. Zooplankton of the southwest coast of india:
656 abundance, composition, temporal and spatial variability in 1987. 1992.
- 657 M Madhupratap, TC Gopalakrishnan, P Haridas, KKC Nair, PN Aravindakshan, G Padmavati, and Shiney Paul.
658 Lack of seasonal and geographic variation in mesozooplankton biomass in the arabian sea and its structure in the
659 mixed layer. *Current science. Bangalore*, 71(11):863–868, 1996a.
- 660 M Madhupratap, S Prasanna Kumar, PMA Bhattathiri, M Dileep Kumar, S Raghukumar, KKC Nair, and N Rama-
661 iah. Mechanism of the biological response to winter cooling in the northeastern arabian sea. *Nature*, 384(6609):
662 549–552, 1996b.

- 663 M Madhupratap, TC Gopalakrishnan, P Haridas, and KKC Nair. Mesozooplankton biomass, composition and
664 distribution in the arabian sea during the fall intermonsoon: implications of oxygen gradients. *Deep Sea Research*
665 *Part II: Topical Studies in Oceanography*, 48(6-7):1345–1368, 2001.
- 666 PA Maheswaran, G Rajesh, C Revichandran, and KKC Nair. Upwelling and associated hydrography along the west
667 coast of india during southwest monsoon, 1999. 2000.
- 668 Douglas Maraun and Jürgen Kurths. Cross wavelet analysis: significance testing and pitfalls. *Nonlinear Processes*
669 *in Geophysics*, 11(4):505–514, 2004.
- 670 JP McCreary, Raghu Murtugudde, Jerome Vialard, PN Vinayachandran, Jerry D Wiggert, Raleigh R Hood,
671 D Shankar, and S Shetye. Biophysical processes in the indian ocean. *Indian Ocean biogeochemical processes*
672 *and ecological variability*, 185:9–32, 2009.
- 673 Julian P McCreary Jr, Pijush K Kundu, and Robert L Molinari. A numerical investigation of dynamics, thermody-
674 namics and mixed-layer processes in the indian ocean. *Progress in Oceanography*, 31(3):181–244, 1993.
- 675 Donald C McNaught. Acoustical determination of zooplankton distribution. In *Proc. 11th Conf. Great lakes Res.*,
676 pages 76–84, 1968.
- 677 A Mukherjee, D Shankar, V Fernando, P Amol, SG Aparna, R Fernandes, GS Michael, ST Khalap, NP Satelkar,
678 Y Agarvadekar, et al. Observed seasonal and intraseasonal variability of the east india coastal current on the
679 continental slope. *Journal of Earth System Science*, 123(6):1197–1232, 2014.
- 680 S Mukhopadhyay, D Shankar, SG Aparna, A Mukherjee, V Fernando, A Kankonkar, S Khalap, NP Satelkar,
681 MG Gaonkar, AP Tari, et al. Observed variability of the east india coastal current on the continental slope
682 during 2009–2018. *Journal of Earth System Science*, 129:1–22, 2020.
- 683 Jerry Mullison. Backscatter estimation using broadband acoustic doppler current profilers-updated. In *Proceedings*
684 *of the ASCE Hydraulic Measurements & Experimental Methods Conference, Durham, NH, USA*, pages 9–12,
685 2017.
- 686 KKC Nair, M Madhupratap, TC Gopalakrishnan, P Haridas, and Mangesh Gauns. The arabian sea: physical
687 environment, zooplankton and myctophid abundance. 1999.
- 688 PV Nair. Primary productivity in the indian seas. *CMFRI Bulletin*, 22:1–63, 1970.
- 689 Lingyun Nie, Jianchao Li, Hao Wu, Wenchao Zhang, Yongjun Tian, Yang Liu, Peng Sun, Zhenjiang Ye, Shuyang
690 Ma, and Qinfeng Gao. The influence of ocean processes on fine-scale changes in the yellow sea cold water mass
691 boundary area structure based on acoustic observations. *Remote Sensing*, 15(17):4272, 2023.
- 692 MD Ohman and H-J Hirche. Density-dependent mortality in an oceanic copepod population. *Nature*, 412(6847):
693 638–641, 2001.

- 694 G Padmavati, P Haridas, KKC Nair, TC Gopalakrishnan, P Shiney, and M Madhupratap. Vertical distribution of
695 mesozooplankton in the central and eastern arabian sea during the winter monsoon. *Journal of Plankton Research*,
696 20(2):343–354, 1998.
- 697 MR Patil, CP Ramamirtham, P Udaya Varma, and CP Nair. Hydrography of the west coast of india during the
698 pre-monsoon period of the year 1962. *Journal of marine biological association of India*, 6(1):151–164, 1964.
- 699 Richard Edward Pieper. *A study of the relationship between zooplankton and high-frequency scattering of underwater*
700 *sound*. PhD thesis, University of British Columbia, 1971.
- 701 SA Piontkovski, R Williams, and TA Melnik. Spatial heterogeneity, biomass and size structure of plankton of the
702 indian ocean: some general trends. *Marine ecology progress series*, pages 219–227, 1995.
- 703 Emmanuel Potiris, Constantin Frangoulis, Alkiviadis Kalampokis, Manolis Ntoumas, Manos Pettas, George Peti-
704 hakis, and Vassilis Zervakis. Acoustic doppler current profiler observations of migration patterns of zooplankton
705 in the cretan sea. *Ocean Science*, 14(4):783–800, 2018.
- 706 SZ Qasim. Biological productivity of the indian ocean. 1977.
- 707 CP Ramamirtham and AVS Murty. Hydrography of the west coast of india during the pre-monsoon period of the
708 year 1962—part 2: in and offshore waters of the konkan and malabar coasts. *Journal of the Marine Biological*
709 *Association of India*, 7(1):150–168, 1965.
- 710 S Ramamurthy. Studies on the plankton of the north kanara coast in relation to the pelagic fishery. *Journal of*
711 *Marine Biological Association of India*, 7(1):127–149, 1965.
- 712 Mehbuba Rehim and Mudassar Imran. Dynamical analysis of a delay model of phytoplankton–zooplankton interac-
713 *tion*. *Applied Mathematical Modelling*, 36(2):638–647, 2012.
- 714 T. P. Rippeth and J. H. Simpson. Diurnal signals in vertical motions on the hebridean shelf. *Limnology and*
715 *Oceanography*, 43:1690–1696, 1998. doi: 10.4319/lo.1998.43.7.1690.
- 716 John H Ryther, John R Hall, Allan K Pease, Andrew Bakun, and Mark M Jones. Primary organic production in
717 relation to the chemistry and hydrography of the western indian ocean 1. *Limnology and Oceanography*, 11(3):
718 371–380, 1966.
- 719 D Sameoto and S Paulowich. The use of 120 khz sonar in zooplankton studies. In *OCEANS'77 Conference Record*,
720 pages 523–528. IEEE, 1977.
- 721 D Shankar and SR Shetye. On the dynamics of the lakshadweep high and low in the southeastern arabian sea.
722 *Journal of Geophysical Research: Oceans*, 102(C6):12551–12562, 1997.
- 723 D Shankar, R Remya, PN Vinayachandran, Abhisek Chatterjee, and Ambica Behera. Inhibition of mixed-layer
724 deepening during winter in the northeastern arabian sea by the west india coastal current. *Climate Dynamics*,
725 47:1049–1072, 2016.

- 726 D Shankar, R Remya, AC Anil, and V Vijith. Role of physical processes in determining the nature of fisheries in the
727 eastern arabian sea. *Progress in Oceanography*, 172:124–158, 2019.
- 728 SR Shetye and AD Gouveia. Coastal circulation in the north indian ocean: Coastal segment (14, sw). John Wiley
729 and Sons, New York, USA, 1998.
- 730 SR Shetye, AD Gouveia, SSC Shenoi, D Sundar, GS Michael, AM Almeida, and K Santanam. Hydrography and
731 circulation off the west coast of india during the southwest monsoon 1987. 1990.
- 732 SR Shetye, AD Gouveia, SSC Shenoi, GS Michael, D Sundar, AM Almeida, and K Santanam. The coastal current
733 off western india during the northeast monsoon. *Deep Sea Research Part A. Oceanographic Research Papers*, 38
734 (12):1517–1529, 1991.
- 735 SR Shetye, AD Gouveia, and SSC Shenoi. Does winter cooling lead to the subsurface salinity minimum off saurashtra,
736 india? *Oceanography of the Indian Ocean*, pages 617–625, 1992.
- 737 Wei Shi and Menghua Wang. Phytoplankton biomass dynamics in the arabian sea from viirs observations. *Journal
738 of Marine Systems*, 227:103670, 2022.
- 739 Greg M Silsbe, Michael J Behrenfeld, Kimberly H Halsey, Allen J Milligan, and Toby K Westberry. The cafe model:
740 A net production model for global ocean phytoplankton. *Global Biogeochemical Cycles*, 30(12):1756–1777, 2016.
- 741 Houssem Smeti, Marc Pagano, Christophe Menkes, Anne Lebourges-Dhaussy, Brian PV Hunt, Valerie Allain, Martine
742 Rodier, Florian De Boissieu, Elodie Kestenare, and Cherif Sammari. Spatial and temporal variability of zooplankton
743 off n ew c aledonia (s outhwestern p acific) from acoustics and net measurements. *Journal of Geophysical
744 Research: Oceans*, 120(4):2676–2700, 2015.
- 745 SL Smith and M Madhupratap. Mesozooplankton of the arabian sea: patterns influenced by seasons, upwelling, and
746 oxygen concentrations. *Progress in Oceanography*, 65(2-4):214–239, 2005.
- 747 Patnaik Sreenivas, KVKRK Patnaik, and KVSR Prasad. Monthly variability of mixed layer over arabian sea using
748 argo data. *Marine Geodesy*, 31(1):17–38, 2008.
- 749 R Subrahmanyam. Studies on the phytoplankton of the west coast of india: Part ii. physical and chemical factors
750 influencing the production of phytoplankton, with remarks on the cycle of nutrients and on the relationship of
751 the phosphate-content to fish landings. In *Proceedings/Indian Academy of Sciences*, volume 50, pages 189–252.
752 Springer, 1959.
- 753 R Subrahmanyam and AH Sarma. Studies on the phytoplankton of the west coast of india. part iii. seasonal variation
754 of the phytoplankters and environmental factors. *Indian Journal of Fisheries*, 7(2):307–336, 1960.
- 755 Laura Ursella, Vanessa Cardin, Mirna Batistić, Rade Garić, and Miroslav Gačić. Evidence of zooplankton vertical
756 migration from continuous southern adriatic buoy current-meter records. *Progress in oceanography*, 167:78–96,
757 2018.

- 758 Laura Ursella, Sara Pensieri, Enric Pallàs-Sanz, Sharon Z Herzka, Roberto Bozzano, Miguel Tenreiro, Vanessa Cardin,
759 Julio Candela, and Julio Sheinbaum. Diel, lunar and seasonal vertical migration in the deep western gulf of mexico
760 evidenced from a long-term data series of acoustic backscatter. *Progress in Oceanography*, 195:102562, 2021.
- 761 V Vijith, PN Vinayachandran, V Thushara, P Amol, D Shankar, and AC Anil. Consequences of inhibition of mixed-
762 layer deepening by the west india coastal current for winter phytoplankton bloom in the northeastern arabian sea.
763 *Journal of Geophysical Research: Oceans*, 121(9):6583–6603, 2016.
- 764 Peter H Wiebe, Charles H Greene, Timothy K Stanton, and Janusz Burczynski. Sound scattering by live zooplankton
765 and micronekton: empirical studies with a dual-beam acoustical system. *The Journal of the Acoustical Society of
766 America*, 88(5):2346–2360, 1990.
- 767 Monika Winder and Daniel E Schindler. Climatic effects on the phenology of lake processes. *Global change biology*,
768 10(11):1844–1856, 2004.
- 769 Karen F Wishner, Marcia M Gowing, and Celia Gelfman. Mesozooplankton biomass in the upper 1000 m in the
770 arabian sea: overall seasonal and geographic patterns, and relationship to oxygen gradients. *Deep Sea Research
771 Part II: Topical Studies in Oceanography*, 45(10-11):2405–2432, 1998.

Table 1: ADCP deployment details at the locations. The temporal resolution is 1 hour, bin size(vertical resolution) 4 m. All ADCPs are operated at 153.3 kHz. The moorings are at a water column depth of 950 - 1200 m on the continental slope and are serviced on yearly basis according to ship availability. The 6th column consists of Reference echo intensity (Er) for each beam, while the 7th column contains the corresponding RSSI conversion factor [Deines, 1999].

| Station (Position; $^{\circ}$ E, $^{\circ}$ N) | Date | | Depth | | | |
|---|------------|------------|-------|------|-------------------|---------------------------|
| | Deployment | Recovery | Ocean | ADCP | Er | Kc |
| Okha (67.47, 22.26) | 01/10/2018 | 01/12/2019 | 996 | 118 | 37 , 37 , 37 , 36 | 0.42 , 0.44 , 0.42 , 0.43 |
| | 01/12/2019 | 04/12/2020 | 1166 | 312 | 39 , 36 , 38 , 36 | 0.42 , 0.44 , 0.42 , 0.43 |
| | 04/12/2020 | 08/03/2022 | 1021 | 144 | 41 , 37 , 38 , 37 | 0.42 , 0.44 , 0.42 , 0.43 |
| | 08/03/2022 | 01/01/2023 | 1019 | 142 | 37 , 38 , 39 , 36 | 0.42 , 0.44 , 0.42 , 0.43 |
| Mumbai (69.24, 20.01) | 09/11/2017 | 29/09/2018 | 1025 | 150 | 36 , 34 , 39 , 42 | 0.40 , 0.40 , 0.40 , 0.40 |
| | 29/09/2018 | 29/11/2019 | 1122 | 125 | 35 , 36 , 39 , 42 | 0.40 , 0.40 , 0.40 , 0.40 |
| | 29/11/2019 | 02/12/2020 | 1143 | 164 | 37 , 34 , 39 , 43 | 0.40 , 0.40 , 0.40 , 0.40 |
| | 02/12/2020 | 06/03/2022 | 1125 | 142 | 36 , 34 , 39 , 42 | 0.40 , 0.40 , 0.40 , 0.40 |
| | 07/03/2022 | 02/01/2023 | 1103 | 158 | 37 , 34 , 40 , 43 | 0.40 , 0.40 , 0.40 , 0.40 |
| Jaigarh (71.12, 17.53) | 27/10/2017 | 27/09/2018 | 1039 | 198 | 32 , 35 , 33 , 32 | 0.45 , 0.45 , 0.45 , 0.45 |
| | 27/09/2018 | 30/10/2019 | 1032 | 164 | 32 , 35 , 33 , 31 | 0.45 , 0.45 , 0.45 , 0.45 |
| | 03/11/2019 | 30/11/2020 | 1142 | 264 | 32 , 36 , 33 , 32 | 0.45 , 0.45 , 0.45 , 0.45 |
| | 30/11/2020 | 05/03/2022 | 1099 | 119 | 33 , 36 , 34 , 32 | 0.45 , 0.45 , 0.45 , 0.45 |
| Goa (72.74, 15.17) | 03/10/2017 | 25/09/2018 | 1000 | 174 | 35 , 37 , 34 , 35 | 0.44 , 0.44 , 0.40 , 0.41 |
| | 25/09/2018 | 16/10/2019 | 969 | 145 | 38 , 36 , 36 , 34 | 0.44 , 0.44 , 0.40 , 0.41 |
| | 16/10/2019 | 29/11/2020 | 966 | 143 | 44 , 38 , 36 , 43 | 0.44 , 0.44 , 0.40 , 0.41 |
| | 29/11/2020 | 03/03/2022 | 985 | 157 | 35 , 40 , 35 , 38 | 0.44 , 0.44 , 0.40 , 0.41 |
| | 03/03/2022 | 05/01/2023 | 984 | 159 | 35 , 38 , 35 , 34 | 0.44 , 0.44 , 0.40 , 0.41 |
| Udupi (74.04, 12.5) | 05/10/2017 | 06/10/2018 | 1028 | 176 | 44 , 46 , 29 , 35 | 0.45 , 0.45 , 0.45 , 0.45 |
| | 06/10/2018 | 18/10/2019 | 1027 | 179 | 32 , 38 , 30 , 36 | 0.45 , 0.45 , 0.45 , 0.45 |
| | 18/10/2019 | 11/12/2020 | 1018 | 168 | 33 , 37 , 31 , 38 | 0.45 , 0.45 , 0.45 , 0.45 |
| | 11/03/2022 | 06/01/2023 | 1036 | 155 | 31 , 32 , 32 , 33 | 0.45 , 0.45 , 0.45 , 0.45 |
| Kollam (75.44, 9.05) | 07/10/2017 | 08/10/2018 | 1174 | 200 | 43 , 55 , 45 , 43 | 0.49 , 0.50 , 0.49 , 0.50 |
| | 08/10/2018 | 20/10/2019 | 1160 | 123 | 49 , 62 , 46 , 46 | 0.49 , 0.50 , 0.49 , 0.50 |
| | 20/10/2019 | 13/12/2020 | 1209 | 176 | 52 , 61 , 54 , 55 | 0.49 , 0.50 , 0.49 , 0.50 |
| | 13/12/2020 | 13/03/2022 | 1129 | 91 | 49 , 51 , 46 , 47 | 0.49 , 0.50 , 0.49 , 0.50 |
| | 13/03/2022 | 08/01/2023 | 1149 | 164 | 41 , 48 , 43 , 41 | 0.49 , 0.50 , 0.49 , 0.50 |
| Kanyakumari (77.39, 6.96) | 16/11/2016 | 08/10/2017 | 1096 | 252 | 37 , 36 , 37 , 37 | 0.42 , 0.44 , 0.42 , 0.43 |
| | 08/10/2017 | 10/10/2018 | 1055 | 181 | 32 , 34 , 38 , 35 | 0.45 , 0.45 , 0.45 , 0.45 |
| | 10/10/2018 | 22/10/2019 | 1075 | 180 | 36 , 34 , 39 , 36 | 0.45 , 0.45 , 0.45 , 0.45 |
| | 22/10/2019 | 14/12/2020 | 1060 | 167 | 33 , 35 , 36 , 35 | 0.45 , 0.45 , 0.45 , 0.45 |
| | 14/12/2020 | 14/03/2022 | 1184 | 287 | 34 , 36 , 36 , 35 | 0.45 , 0.45 , 0.45 , 0.45 |

Table 2:

Volumetric samples of zooplankton of various stations. The sampling depth range is standardised for later years for bin range of 0–25m, 25–50m, 50–75m, 75–100m, 100–150m. The abbreviations are in the following manner: Okha (O), Mumbai (M), Jaigarh (J), Goa (G), Udupi (U), Kollam (K), Kanyakumari (KK); The number tags corresponds to particular cruise of a station.

| Sample number | Tag | Lat($^{\circ}$ N) | Lon($^{\circ}$ E) | Date | Time (IST) | Sampling depth range (m) |
|---------------|-----|--------------------|--------------------|-----------|------------|-------------------------------|
| 1-3 | G1 | 15.18 | 72.79 | 25 Sep 18 | 452 | 50–25, 100–50, 150–100 |
| 4-6 | G2 | 15.16 | 72.71 | 25 Sep 18 | 2108 | 50–25, 100–50, 150–100 |
| 7-10 | G2 | 15.16 | 72.71 | 25 Sep 18 | 2137 | 40–20, 60–40, 80–60, 100–80 |
| 11-14 | J1 | | | 26 Sep 18 | 2000 | 40–20, 60–40, 80–60, 100–80 |
| 15-17 | J2 | | | 27 Sep 18 | 2000 | 50–25, 100–50, 150–100 |
| 18-21 | J2 | | | 27 Sep 18 | 2100 | 40–20, 60–40, 80–60, 100–80 |
| 22-25 | M1 | 20 | 69.19 | 28 Sep 18 | 2135 | 40–20, 60–40, 80–60, 100–80 |
| 26-27 | M1 | 20 | 69.19 | 28 Sep 18 | 2205 | 50–25, 100–50 |
| 28-29 | M2 | 20.01 | 69.2 | 29 Sep 18 | 2035 | 50–25, 100–50 |
| 30-33 | M2 | 20.01 | 69.2 | 29 Sep 18 | 2057 | 40–20, 60–40, 80–60, 100–80 |
| 34-37 | U1 | | | 5 Oct 18 | 2000 | 40–20, 60–40, 80–60, 100–80 |
| 38-40 | U1 | | | 5 Oct 18 | 2100 | 50–25, 100–50, 150–100 |
| 41-43 | U2 | | | 6 Oct 18 | 2000 | 50–25, 100–50, 150–100 |
| 44-47 | U2 | | | 6 Oct 18 | 2100 | 40–20, 60–40, 80–60, 100–80 |
| 48-51 | K1 | 9.06 | 75.42 | 8 Oct 18 | 421 | 40–20, 60–40, 80–60, 100–80 |
| 52-54 | K1 | 9.06 | 75.42 | 8 Oct 18 | 449 | 50–25, 100–50, 150–100 |
| 55-56 | K2 | 9.04 | 75.4 | 8 Oct 18 | 2027 | 50–25, 100–50 |
| 57-60 | K2 | 9.04 | 75.4 | 8 Oct 18 | 2045 | 40–20, 60–40, 80–60, 100–80 |
| 61-64 | G2 | 15.16 | 72.74 | 16 Oct 19 | 829 | 50–25, 75–50, 100–75, 150–100 |
| 65-67 | G3 | 15.16 | 72.74 | 16 Oct 19 | 1812 | 50–25, 75–50, 100–75 |
| 68-70 | K2 | 9.02 | 75.42 | 20 Oct 19 | 840 | 50–25, 75–50, 100–75 |
| 71-74 | K3 | 9.04 | 75.43 | 20 Oct 19 | 1934 | 50–25, 75–50, 100–75, 150–100 |
| 75-78 | KK1 | | | 22 Oct 19 | 742 | 50–25, 75–50, 100–75, 150–100 |
| 79-82 | KK2 | | | 22 Oct 19 | 1925 | 50–25, 75–50, 100–75, 150–100 |
| 83-86 | J1 | | | 30 Oct 19 | 324 | 50–25, 75–50, 100–75, 150–100 |
| 87-89 | J2 | | | 4 Nov 19 | 946 | 75–50, 100–75, 150–100 |
| 90-92 | M2 | 19.98 | 69.22 | 29 Nov 19 | 1434 | 50–25, 75–50, 100–75 |
| 93-96 | M3 | 20.01 | 69.23 | 30 Nov 19 | 958 | 50–25, 75–50, 100–75, 150–100 |
| 97-100 | O1 | 22.24 | 67.49 | 1 Dec 19 | 937 | 50–25, 75–50, 100–75, 150–100 |
| 101 | O2 | 22.25 | 67.46 | 1 Dec 19 | 1957 | 150–100 |
| 102-105 | G3 | 15.68 | 73.22 | 28 Nov 20 | 930 | 50–25, 75–50, 100–75, 150–100 |
| 105-108 | G4 | 15.32 | 73.22 | 29 Nov 20 | 1558 | 50–25, 75–50, 100–75, 150–100 |
| 108-110 | J2 | 17.85 | 71.21 | 30 Nov 20 | 1458 | 75–50, 100–75, 150–100 |
| 111-114 | J3 | 17.91 | 71.21 | 1 Dec 20 | 1052 | 50–25, 75–50, 100–75, 150–100 |
| 115-118 | M4 | 20.03 | 69.38 | 2 Dec 20 | 2016 | 50–25, 75–50, 100–75, 150–100 |
| 119-00 | O2 | 22.41 | 67.8 | 4 Dec 20 | 953 | 150–100 |
| 120-123 | O3 | 22.41 | 67.79 | 4 Dec 20 | 2011 | 50–25, 75–50, 100–75, 150–100 |
| 124-127 | K3 | 9.11 | 75.72 | 12 Dec 20 | 2335 | 50–25, 75–50, 100–75, 150–100 |
| 128-131 | K4 | 9.06 | 75.74 | 13 Dec 20 | 1507 | 50–25, 75–50, 100–75, 150–100 |
| 132-134 | KK1 | 7.62 | 77.63 | 14 Dec 20 | 1226 | 50–25, 75–50 |
| 135-138 | KK2 | 7.62 | 77.63 | 14 Dec 20 | 2047 | 50–25, 75–50, 100–75, 150–100 |
| 139-142 | G4 | 15.32 | 73.21 | 3 Mar 22 | 823 | 50–25, 75–50, 100–75, 150–100 |
| 143-146 | G5 | 15.68 | 73.21 | 4 Mar 22 | 1030 | 50–25, 75–50, 100–75, 150–100 |
| 147-150 | M5 | 19.99 | 69.23 | 7 Mar 22 | 957 | 50–25, 75–50, 100–75, 150–100 |
| 151-154 | O3 | 22.24 | 67.5 | 8 Mar 22 | 806 | 50–25, 75–50, 100–75, 150–100 |
| 155-158 | U3 | 12.5 | 74.04 | 12 Mar 22 | 1156 | 50–25, 75–50, 100–75, 150–100 |
| 159-160 | K4 | 9.04 | 75.42 | 13 Mar 22 | 1027 | 50–25, 75–50, 100–75 |
| 161-164 | KK3 | 6.97 | 77.4 | 15 Mar 22 | 1220 | 50–25, 75–50, 100–75, 150–100 |

Table 3:

The mean, standard deviation at 40 and 104 m of biomass at 7 mooring sites and their difference is tabulated. All units are in $mg\ m^{-3}$.

| | 40 m | | 104 m | | difference |
|-------------|--------|-------|--------|-------|------------|
| | Mean | std | Mean | std | |
| Okha | 230.42 | 22.84 | 151.68 | 25.58 | 78.74 |
| Mumbai | 272.86 | 34.95 | 182.24 | 30.34 | 90.62 |
| Jaigarh | 278.45 | 36.52 | 182.96 | 48.89 | 95.49 |
| Goa | 235.22 | 30.34 | 163.02 | 36.54 | 72.2 |
| Udupi | 247.81 | 34.37 | 169.37 | 38.8 | 78.43 |
| Kollam | 272.56 | 54.94 | 198.89 | 50.08 | 73.67 |
| Kanyakumari | 207.07 | 30.42 | 167.63 | 20.89 | 39.44 |

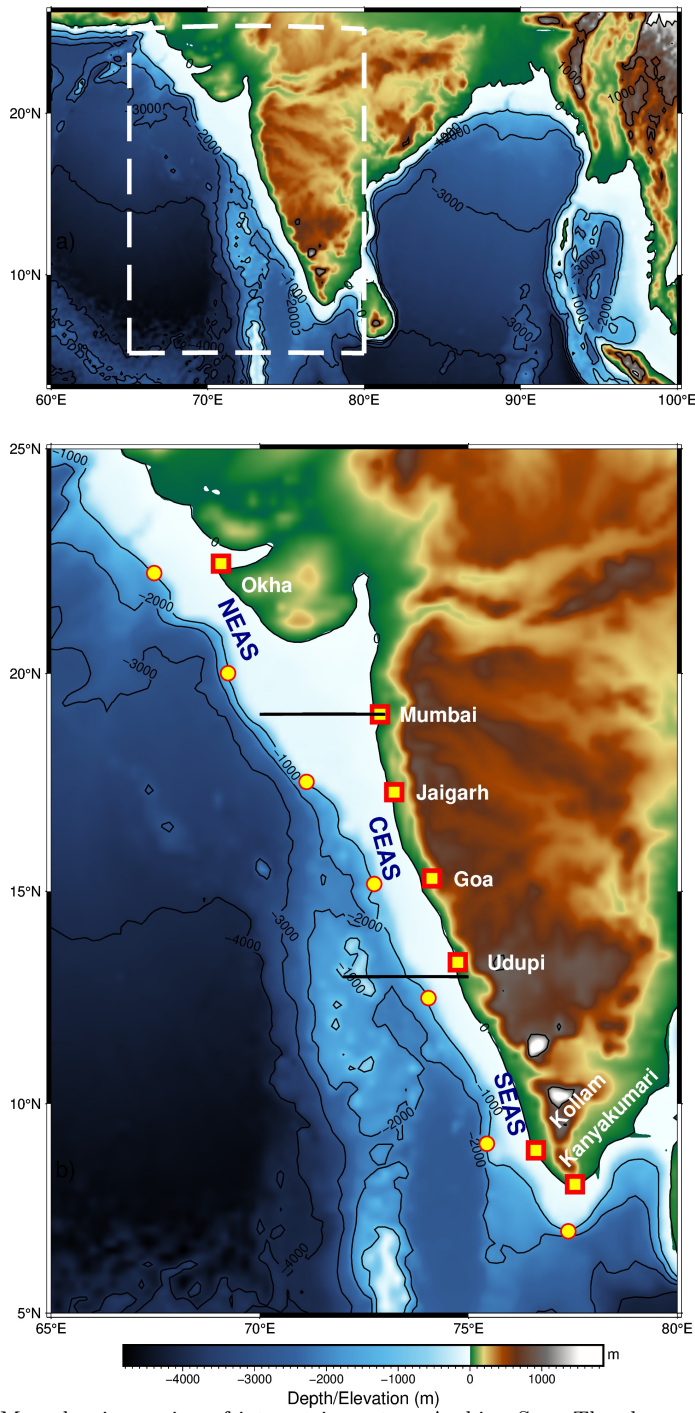


Figure 1: Map showing region of interest in eastern Arabian Sea. The slope moorings are deployed at ~ 1000 m depth as shown in the bathymetry contour. Note the increase in shelf width as we go poleward along the coast. The mooring sites off Okha and Mumbai are in Northern EAS; Jaigarh and Goa in Central EAS while Kollam and Kanyakumari are at Southern EAS. Udupi is situated at the transition zone of Central and Southern EAS.

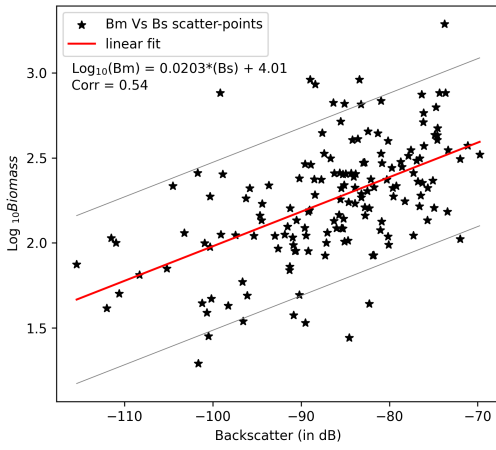


Figure 2: The linear fit line of Biomass (\log_{10} scale) and backscattering strength (in dB). The linear fit line is within the error range of previous result of [Aparna et al., 2022] (contained 67 data points) onto which latest zooplankton volumetric sample data (159 data points) is appended. The first standard deviation of \log_{10} Biomass is ± 0.49 , which results in the backscatter range of 48.58 dB encompassing the entire backscatter range. It signifies the robustness of zooplankton biomass dependency on ADCP measured backscattering strength.

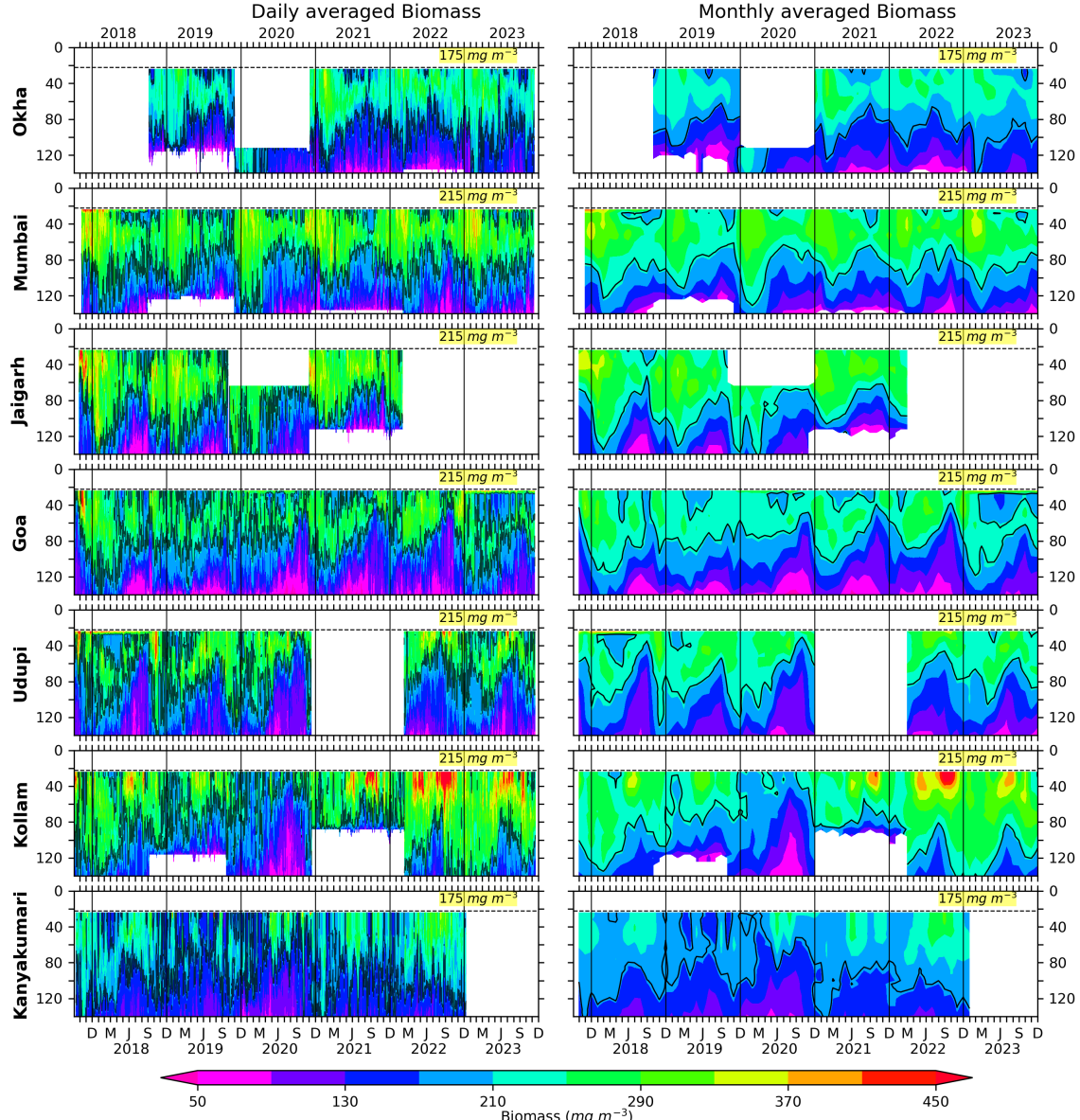


Figure 3: The Daily and monthly averaged biomass for EAS moorings, north (top) to south (bottom). The black contours are marking of 175 mg m^{-3} biomass for Okha and Kanyakumari; 200 mg m^{-3} for Jaigarh and Udupi; 215 mg m^{-3} for Mumbai, Goa and Kollam. The biomass contours are distinct and different based on the physico-chemical parameters and the one that best explains seasonality at respective location. The top 10 % of data is discarded due to echo noise. The dashed line at 22 m marks the top-depth of first bin i.e, 24 m.

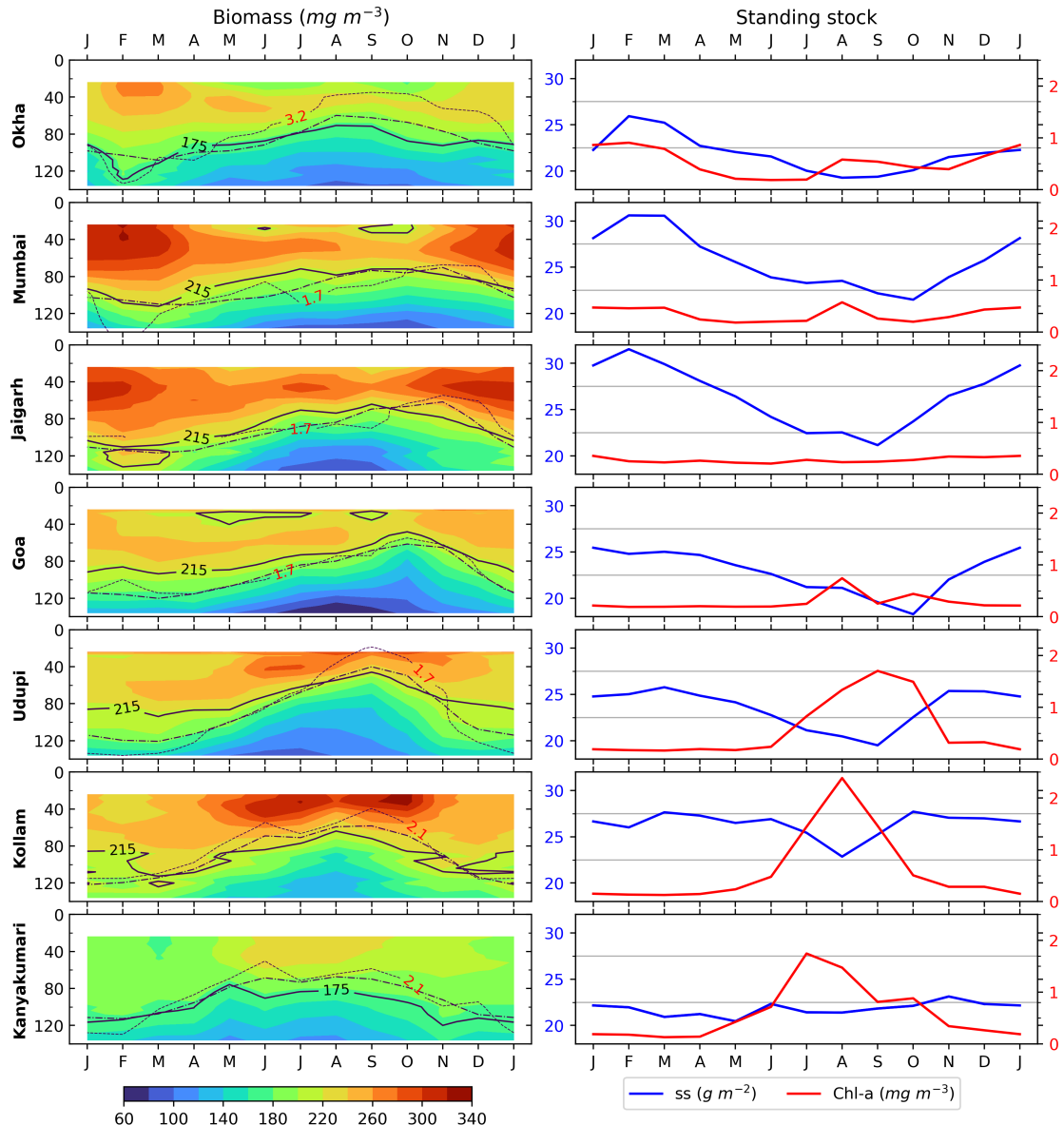


Figure 4: Monthly climatology of zooplankton biomass is shown in left panels for 7 locations, (top to bottom is southward). The D175, D200 & D215 are shown in solid lines; dashed line represents the depth of 23 C isotherm; oxygen contours are shown in dotted lines and labeled for each mooring. The right set of panel plots is showing ZSS and chlorophyll climatology for corresponding locations.

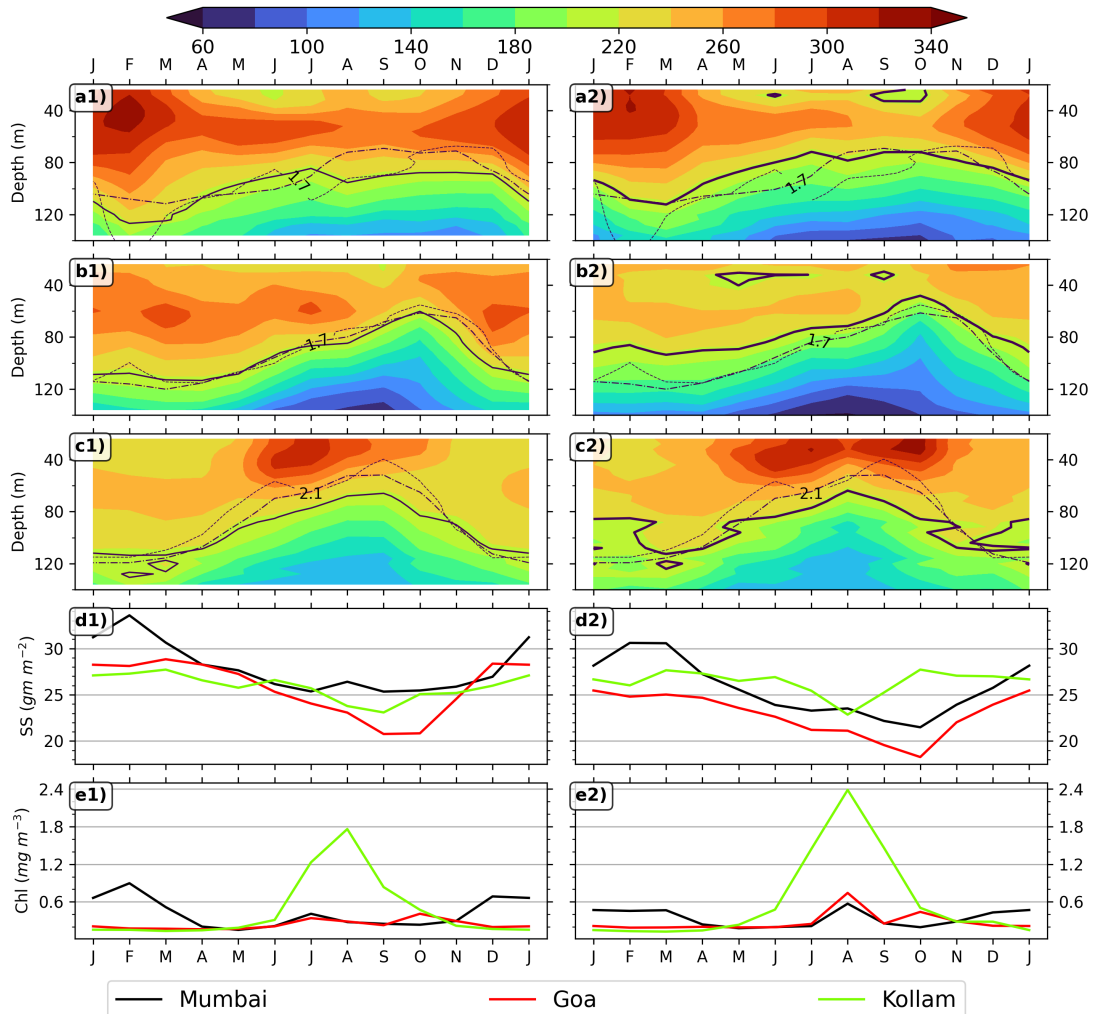


Figure 5: Monthly climatology of zooplankton biomass is shown in left panels for 3 locations which were earlier used in [Aparna et al., 2022]; a1, b1 & c1 is the biomass climatology for Mumbai, Goa and Kollam, d1 is for ZSS climatology, e1 is for chlorophyll biomass climatology; a2, b2, c2, d2 & e2 is same but based on data from 2017 to 2023. The D215 is shown in solid line. The dashed line represents the depth of 23 °C isotherm; oxygen contours are shown in dotted lines and labeled for each mooring.

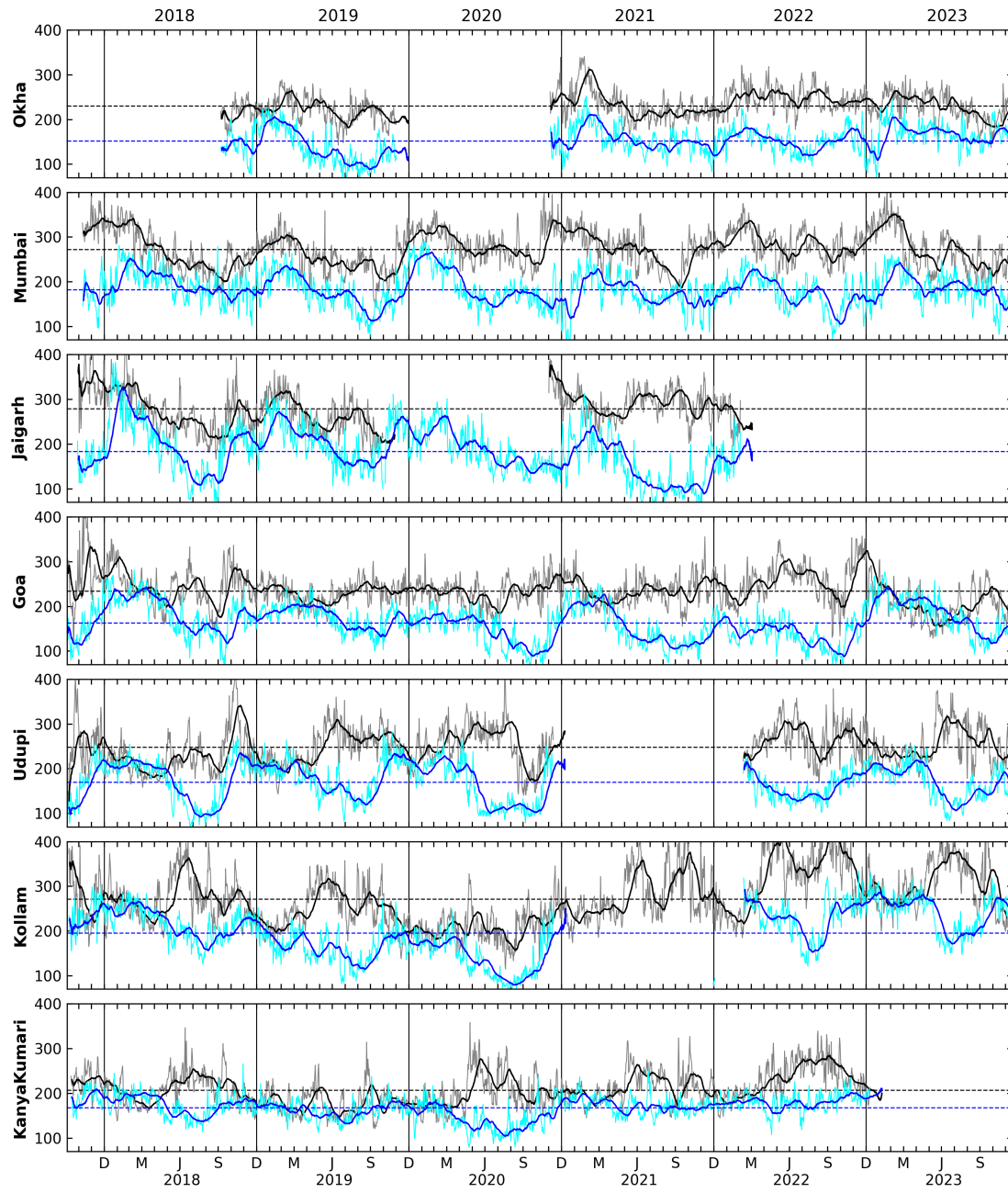


Figure 6: The daily biomass at depth of 40 m and 104 m for all locations shown by grey and cyan curves. The black and blue lines shows the 30 day rolling averaged biomass at 40 and 104 m, respectively. Notice the bursts seen in the daily data ranging from few days to weeks.

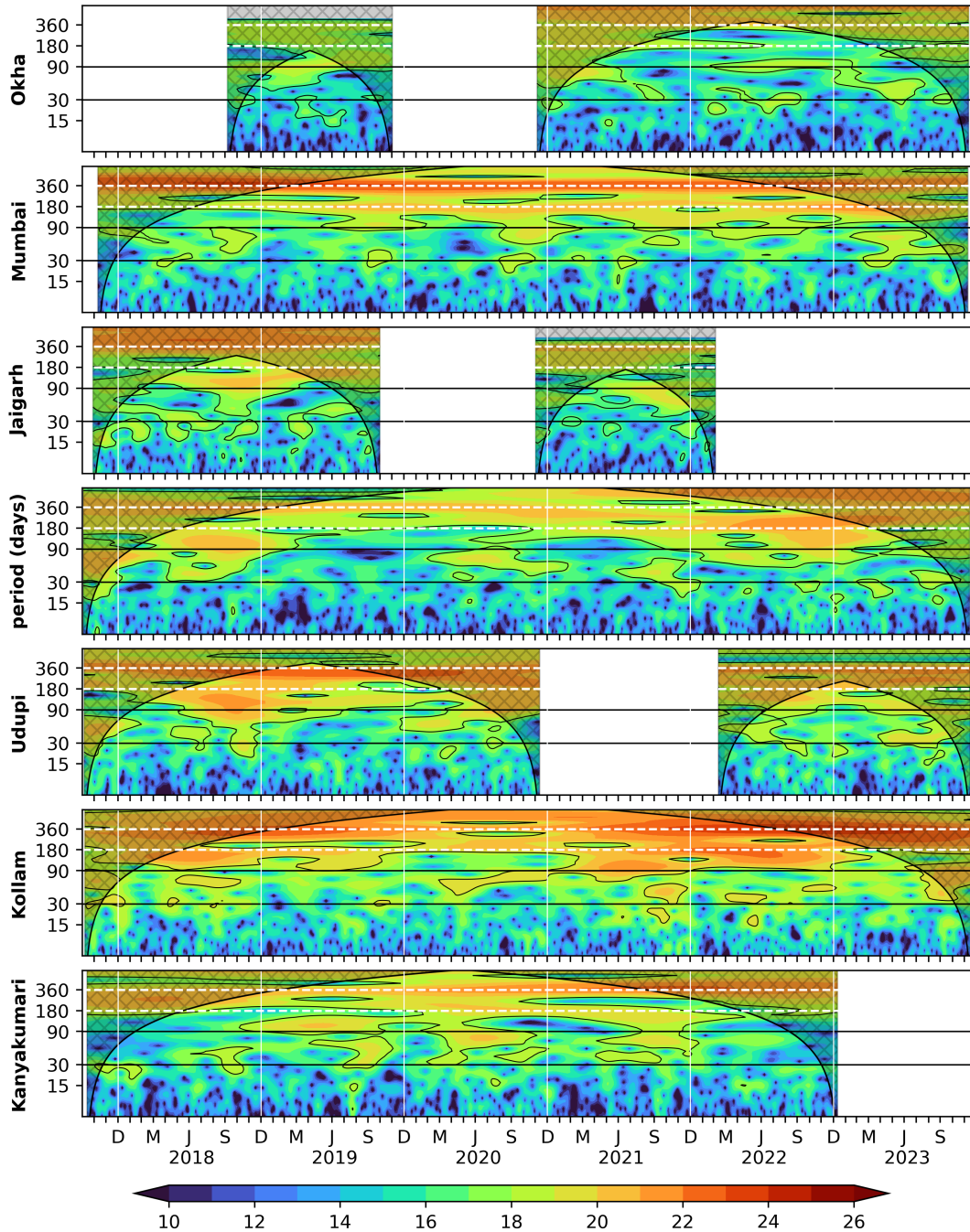


Figure 7: Wavelet power spectra (Morlet) of the 40 m zooplankton biomass plotted against time as abscissa and period in days as ordinate. The wavelet power is in \log_2 scale, the 95 % significance is marked in black contours; the cross-shaded region falls under cone of influence. Vertical white lines separates years.

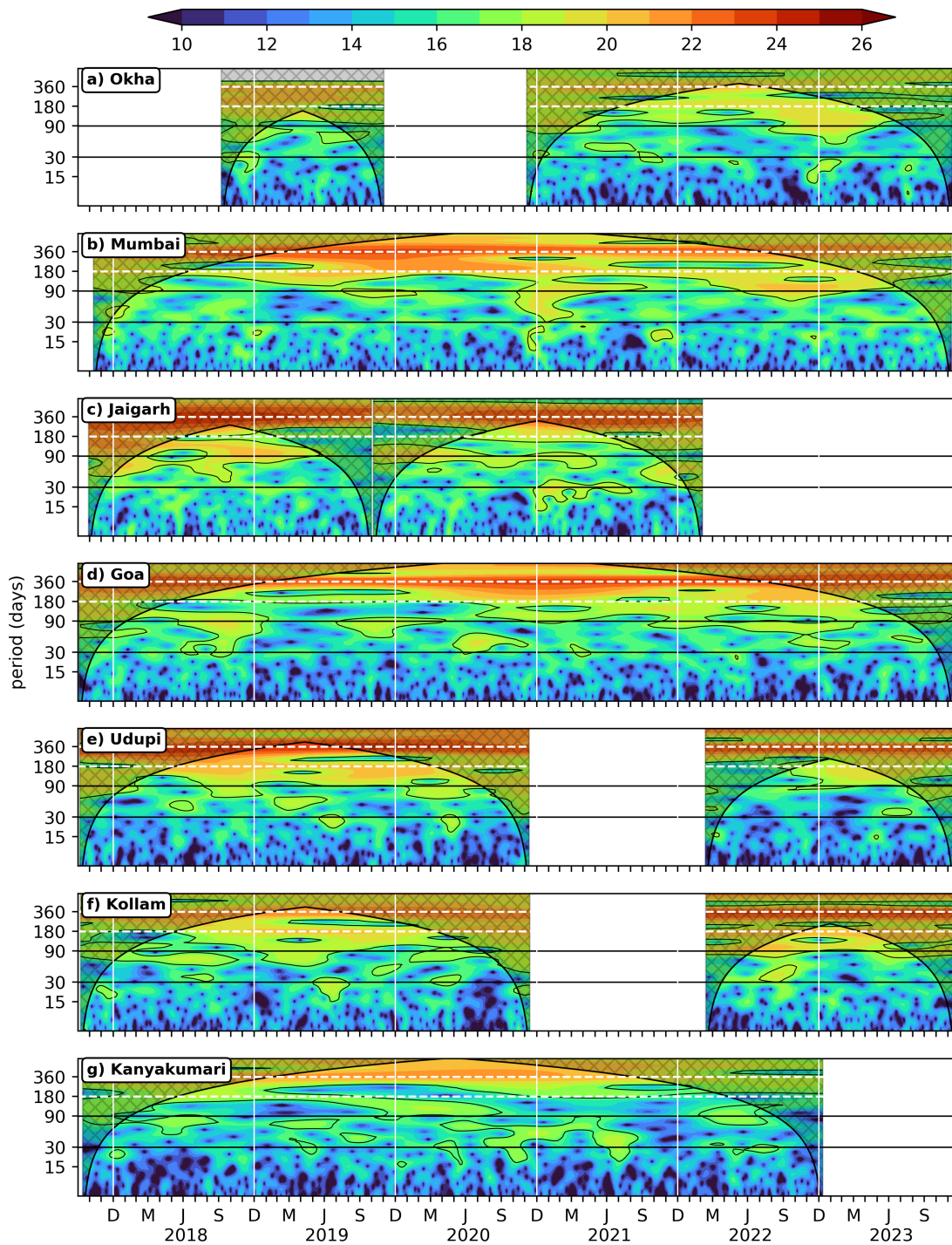


Figure 8: Wavelet power spectra (Morlet) of the 104 m zooplankton biomass plotted against time as abscissa and period in days as ordinate. The wavelet power is in log₂ scale, the 95 % significance is marked in black contours; the cross-shaded region falls under cone of influence. The vertical white lines separates years.

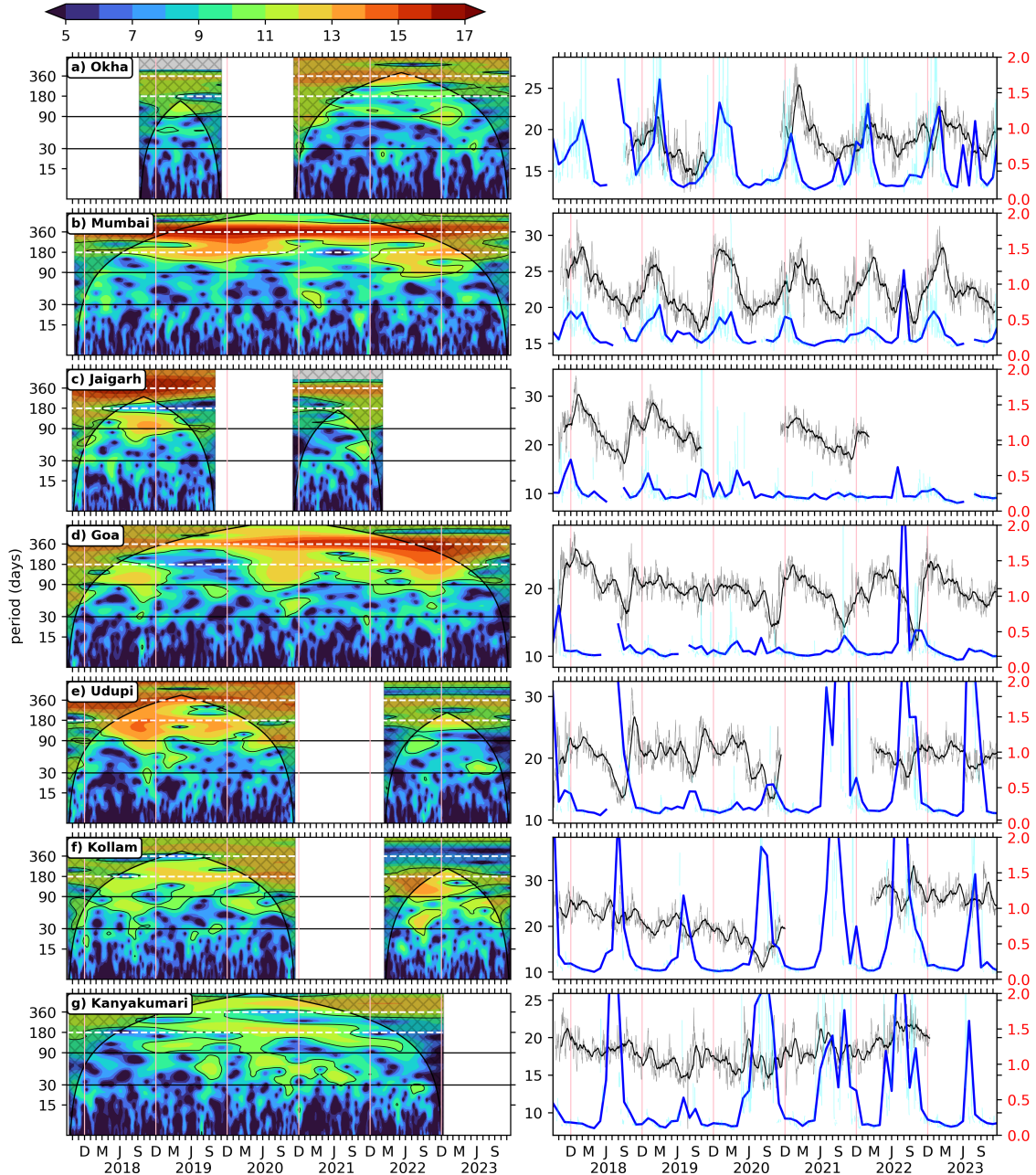


Figure 9: Wavelet power spectra (Morlet) of zooplankton standing stock plotted against time as abscissa and period in days as ordinate. The wavelet power is in log₂ scale, the 95 % significance is marked in black contours; The vertical white lines separates years. The right side panel shows the ZSS time series of 30 day rolling mean data (black)overlaid upon daily data (Grey). The 30 day rolling mean data of chlorophyll (solid blue line) is plotted over its daily data (cyan).

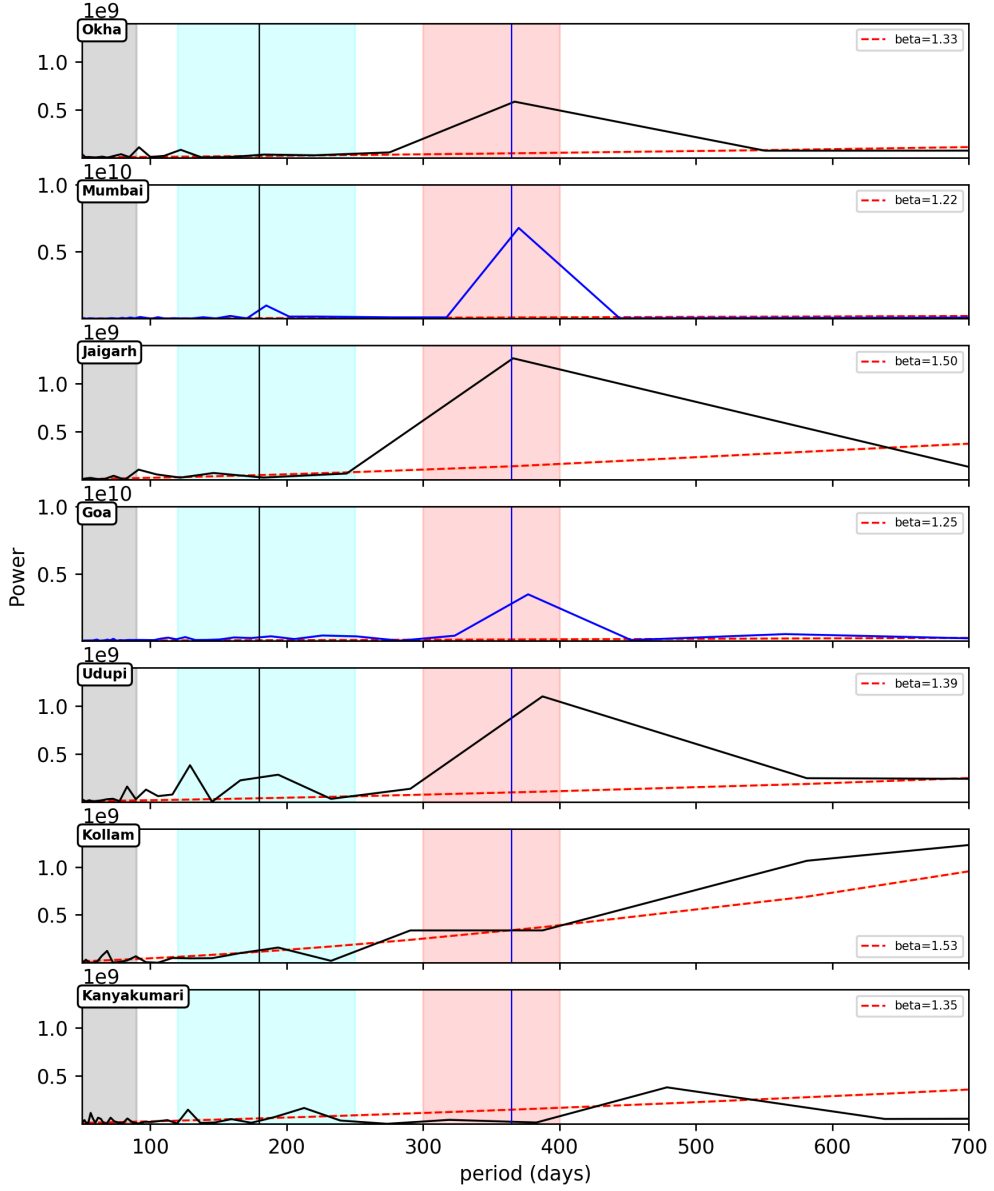


Figure 10: FFT of the ZSS time series data. On the event of discontinuity in data record, the longest available of respective location is considered for analysis. The black (blue) curve is fft power with scale 10^9 (10^{10}). The Grey, cyan and pink spans the intra-seasonal, seasonal and annual bands, respectively. The red dashed curved is the red noise spectra which depends on the number of records of each location, and beta determines power contribution of the higher and lower frequencies. The vertical blue line marks the annual cycle.

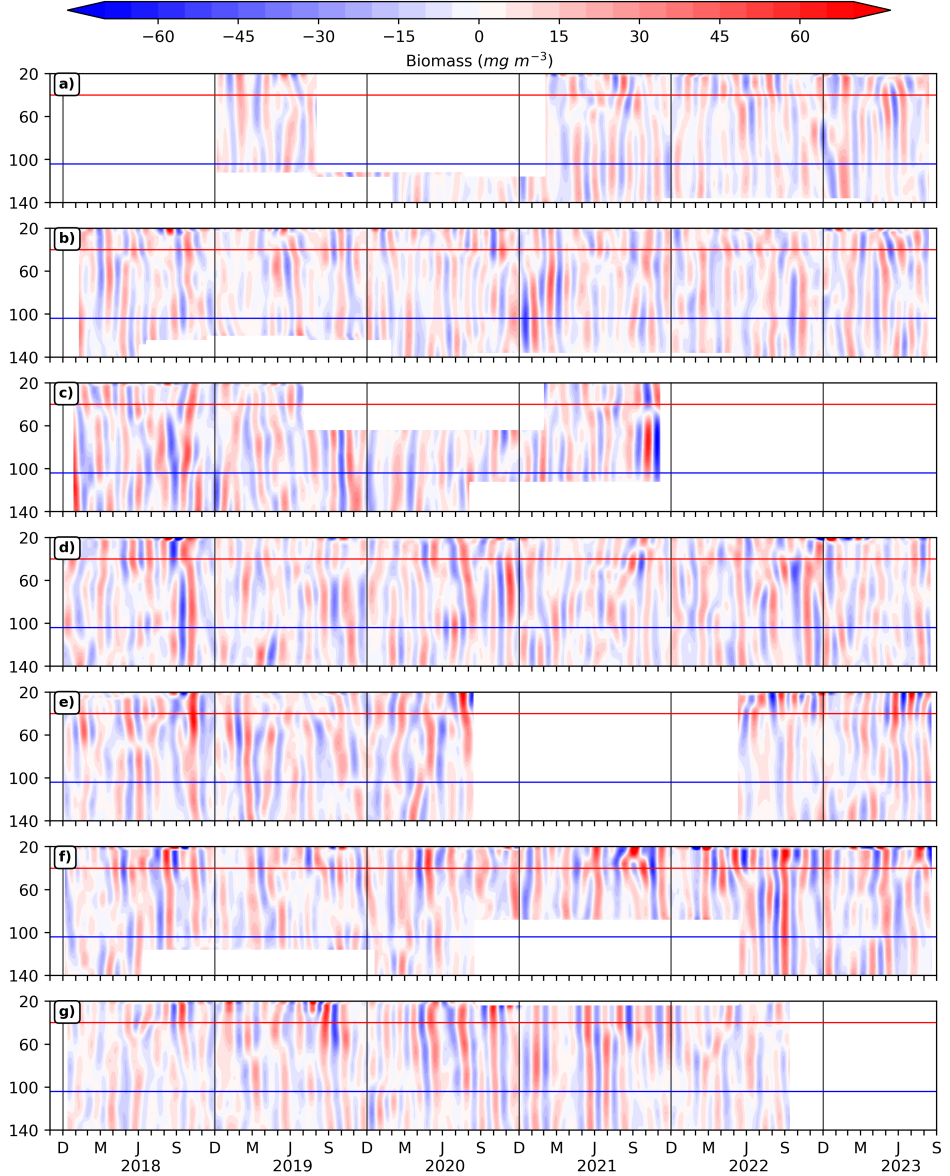


Figure 11: Biomass variation found in the scale of 30 to 90 days period (Intra-seasonal band as it is within a season) is obtained using a lanczos band pass filter. The horizontal black and blue lines is for 40 and 104 m respectively; vertical black lines separate the years. The dashed line at 22 m marks the top-depth of first bin i.e, 24 m. Intraseasonal variability is seen throughout the record and the variability is stronger during August to November.

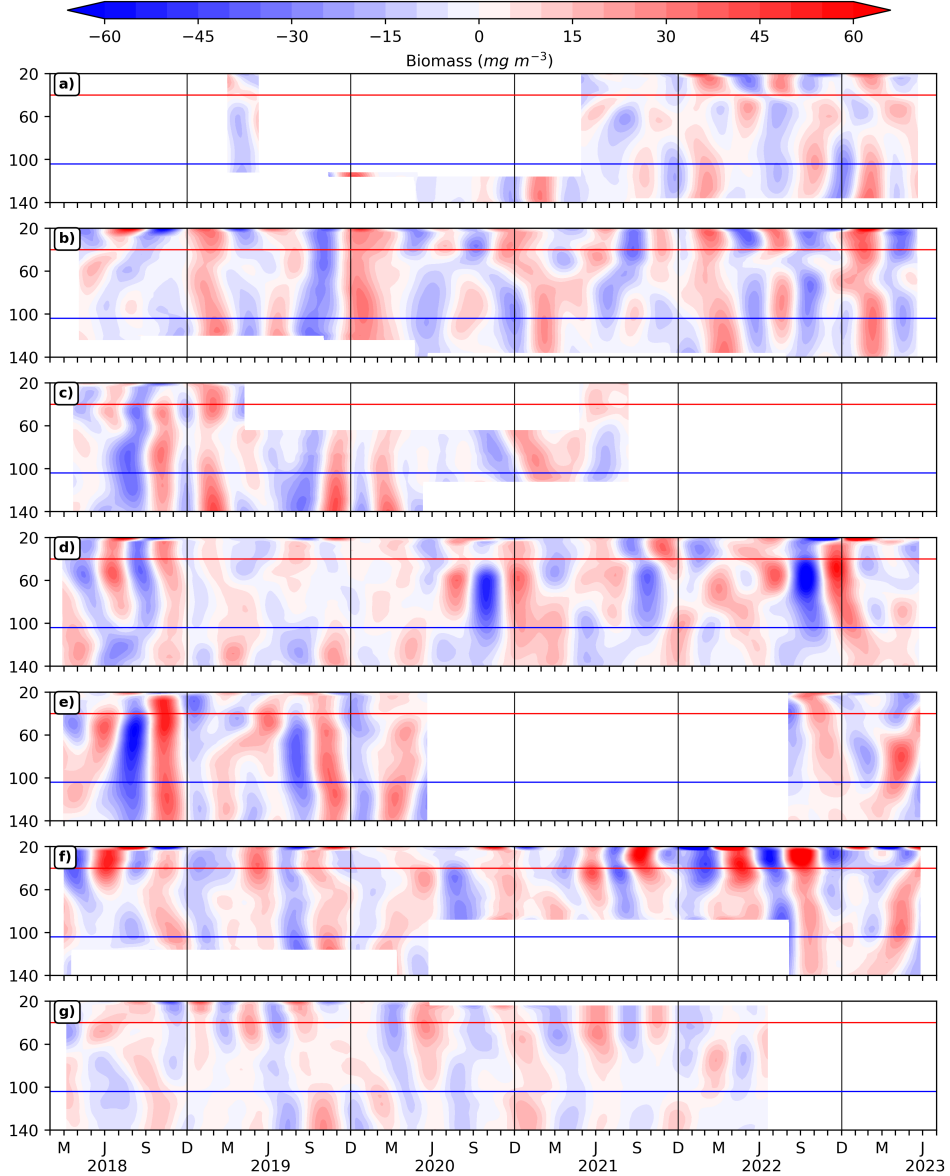


Figure 12: The biomass variation occurring in 100 to 250 days period (between the seasons and within a year record or intra-annual band) is obtained using a band pass filter. The horizontal black and blue lines is for 40 and 104 m respectively; vertical black lines separate the years. The dashed line at 22 m marks the top-depth of first bin i.e, 24 m.